AD-A089 377 AERONAUTICAL RESEARCH LABS MELBOURNE (AUSTRALIA) F/G 14/2
AN INTRODUCTION TO DYNAMIC DERIVATIVES (3) METHODS OF OSCILLATI--ETC(U)
APR 79 G F FORSYTH
UNCLASSIFIED ARL/AERO NOTE-390 NL

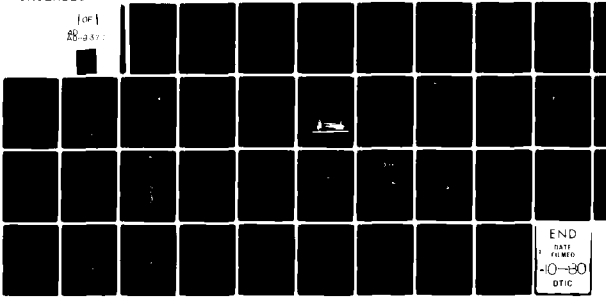

ARL-AERO-NOTE-390

AR-001-724

DEPARTMENT OF DEFENCE

DEFENCE SCIENCE AND TECHNOLOGY ORGANISATION

AERONAUTICAL RESEARCH LABORATORIES

MELBOURNE, VICTORIA

AERODYNAMICS NOTE 390

AN INTRODUCTION TO DYNAMIC DERIVATIVES (3) METHODS OF OSCILLATING MODELS IN PITCH AND YAW IN A 530 BY 810 MILLIMETRE TRANSONIC WIND TUNNEL

by

G. F. FORSYTH

Approved for Public Release.

COPY No 21

APRIL 1979

AR-001-724

DEPARTMENT OF DEFENCE
DEFENCE SCIENCE AND TECHNOLOGY ORGANISATION
AERONAUTICAL RESEARCH LABORATORIES

AERODYNAMICS NOTE 390

AN INTRODUCTION TO DYNAMIC DERIVATIVES (3) METHODS OF OSCILLATING MODELS IN PITCH AND YAW IN A 530 BY 810 MILLIMETRE TRANSONIC WIND TUNNEL.

by

G. F. FORSYTH

SUMMARY

Mechanisms are considered which allow models to be oscillated in pitch and yaw during wind tunnel tests to measure dynamic derivatives. Types of pivots, motion producing linkages and connecting linkages are described as applicable in a 530 by 810 millimetre Transonic Tunnel.

POSTAL ADDRESS: Chief Superintendent, Aeronautical Research Laboratories,
Box 4331, P.O., Melbourne, Victoria, 3001, Australia.

DOCUMENT CONTROL DATA SHEET

Security classification of this page: Unclassified

1. Document Numbers
   (a) AR Number:
   AR-001-724
   (b) Document Series and Number:
   Aerodynamics Note 390
   (c) Report Number:
   ARL-Aero-Note-390

2. Security Classification
   (a) Complete document:
   Unclassified
   (b) Title in isolation:
   Unclassified
   (c) Summary in isolation:
   Unclassified

3. Title: AN INTRODUCTION TO DYNAMIC DERIVATIVES (3). METHODS OF OSCILLATING MODELS IN PITCH AND YAW IN A 530 BY 810 MILLIMETRE TRANSONIC WIND TUNNEL

4. Personal Author(s):
   G. F. Forsyth

5. Document Date:
   April, 1979

6. Type of Report and Period Covered:

7. Corporate Author(s):
   Aeronautical Research Laboratories

8. Reference Numbers
   (a) Task:

9. Cost Code:
   54 7721

   (b) Sponsoring Agency:

10. Imprint
    Aeronautical Research Laboratories,
    Melbourne

11. Computer Program(s)
    (Title(s) and language(s)):

12. Release Limitations (of the document)
    Approved for public release

12-0. Overseas:	N.O.		P.R.	1	A		B		C		D		E	

13. Announcement Limitations (of the information on this page):
    No limitation

14. Descriptors:

Wind tunnel models	Pitching	
Wind tunnels	Yaw	
Oscillations	Linkages	
Pivots		

15. Cosati Codes:
    1201
    1402
    2011

16. *ABSTRACT*

Mechanisms are considered which allow models to be oscillated in pitch and yaw during wind tunnel tests to measure dynamic derivatives. Types of pivots, motion producing linkages and connecting linkages are described as applicable in a 530 by 810 millimetre Transonic Tunnel.

CONTENTS

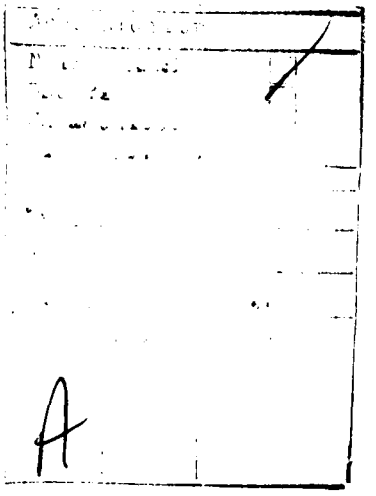

NOTATION

C_x, C_y, C_z	aero-normal coefficient of the force X, Y or Z given by
C_x	$= X/(\frac{1}{2}\rho_e V_e^2 S)$, for example
C_m	aero-normal coefficient of the moment m $= m/(\frac{1}{2}\rho_e V_e^2 S l_0)$
$C_{x\dot{\alpha}}$, etc.	derivatives based on aero-normal force coefficients and aero-normal variables $= \frac{\partial C_x}{\partial \dot{\bar{\alpha}}} = \frac{1}{\frac{1}{2}\rho_e V_e^2 S} \frac{\partial X}{\partial \dot{\bar{\alpha}}} = \frac{1}{\frac{1}{2}\rho_e V_e l_0 S} \frac{\partial X}{\partial \dot{\alpha}}$
$C_{m\dot{\alpha}}$, etc.	derivatives based on aero-normal moment coefficients and aero-normal variables $= \frac{\partial C_m}{\partial \dot{\bar{\alpha}}} = \frac{1}{\frac{1}{2}\rho_e V_e^2 S l_0} \frac{\partial m}{\partial \dot{\bar{\alpha}}} = \frac{1}{\frac{1}{2}\rho_e V_e S l_0^2} \frac{\partial m}{\partial \dot{\alpha}}$
I_y	moment of inertia about a y-axis
j	$\sqrt{-1}$
K	a constant, derivatives used as spring rates, K_θ & $K_{\dot{\theta}}$
l_0	representative length
m	pitching moment about a y-axis
m_e	mass in stability axes
$\bar{m}_e = \mu$	aero-normal mass
m_α	pitching moment incidence derivative
q	pitch rate; equal to $\dot{\theta}$
S	representative area
T	Tension of Torque; amplitude is T_0
V_e	datum velocity
α	incidence angle, usually sine definition
Δ	change
η	pitch motivator deflection
θ	pitch angle
θ_c	cable pitch angle
μ	density parameter, aero-normal mass
λ	real part of an exponential solution
ρ_e	datum air density
ω	frequency in radians/second
ω_0	natural frequency, ω for undamped system

Superscript bar means aero-normal terms

1. INTRODUCTION

The measurement of unsteady aerodynamic forces in the wind tunnel is a problem of different nature from that of measuring steady or static forces. With unsteady forces the technique to be employed depends more critically on the quantity to be measured. A literature survey has therefore been conducted to determine which quantities should be measured and the appropriate methods.

The present field of interest lies at Mach numbers between $M_0 = 0{\cdot}4$ and $M_0 = 1{\cdot}4$. Quantities such as ground effects which are not relevant in this range have not been considered and only methods suitable for the ARL Transonic Wind Tunnel have been investigated.

An earlier Note in this Series (86) (A.N. 330) determined a list of quantities which appear to be of interest under these conditions (Table 1). Some of these quantities are measurable by single mode angular oscillations (* on Table 1) and the measurement of these will be considered in this note. This group involves what is termed the direct derivatives with respect to α, $\dot{\alpha}$, q, β, $\dot{\beta}$ and r. Indirect, or cross, derivatives such as Cl_β, where the first and second subscript represent quantities about different axes, will not be treated here and neither will rolling derivatives (e.g. Cl_p).

Schemes for measuring these direct derivatives will be discussed with particular reference to the ARL Transonic Tunnel, the pertinent features of which will first be described. Various schemes will then be considered in turn for each of the types of model used in transonic wind tunnels, (i) full models, usually sting mounted, (ii) half models, usually mounted on one side wall, and (iii) two-dimensional models mounted either between two side walls or two end plates supported by the side walls.

The mathematics of the equations of motion for the systems considered in this Note have already been published (87).

2. THE ARL TRANSONIC WIND TUNNEL

Features of the Aeronautical Research Laboratory's Transonic Wind Tunnel are shown in Figures 1 to 4. The working section is rectangular, approximately 810 millimetres high and 530 millimetres wide. The test section is available in two basic configurations plus combinations of these two. One (Fig. 2) has four slotted walls and all models are sting mounted. The sting is mounted on two movable slides (Fig. 4) in a vertical strut in the diffuser. This section of the diffuser slides back to allow access. The second configuration (Fig. 3) uses solid side walls with slotted top and bottom sections. The centre strut remains in position but incidence change may now also be accomplished by rotation of the side-windows.

Neither of these two incidence mechanisms has response fast enough to measure dynamic derivatives on the static balances. A small free oscillation rig similar to that used by Sandia Corporation (20) exists and is discussed in this Note. A dampometer (55) has recently been calibrated (56). No other dynamic equipment is currently used in this tunnel. The capability of measuring wider ranges of derivatives is currently being investigated and has led to this series of Notes.

Other data on the wind tunnel are given in Table 2.

3. ALPHA, BETA MODES IN THE WIND TUNNEL TESTS OF MODELS WITH MORE THAN ONE DEGREE OF FREEDOM

3.1 Free Models

It is possible to "fly" a model in the wind tunnel either completely un-constrained or connected solely by an umbilical cord to provide power, fuel or data exchange. At low speeds

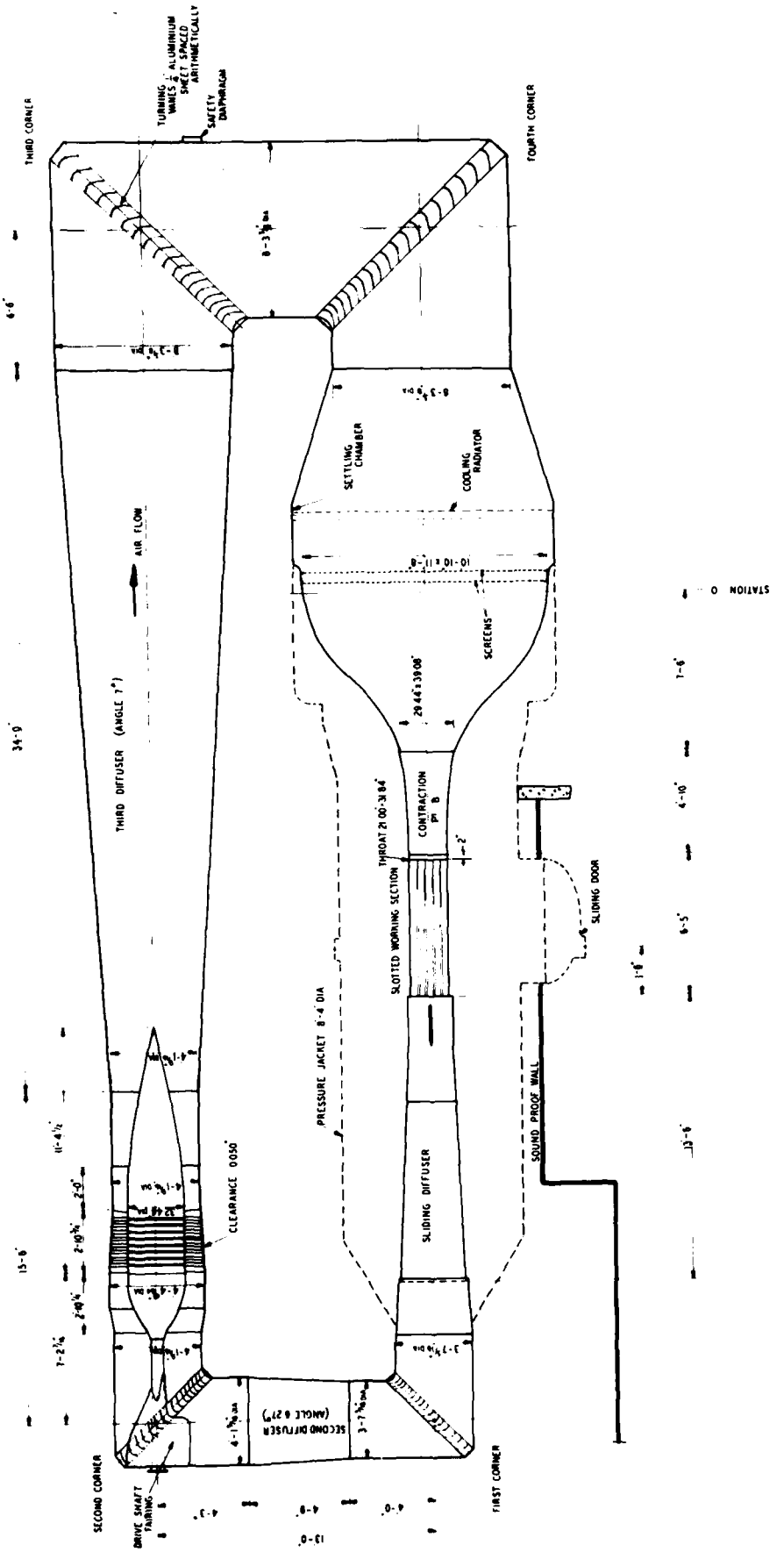

FIG 1. AERODYNAMIC OUTLINE OF TRANSONIC WIND TUNNEL

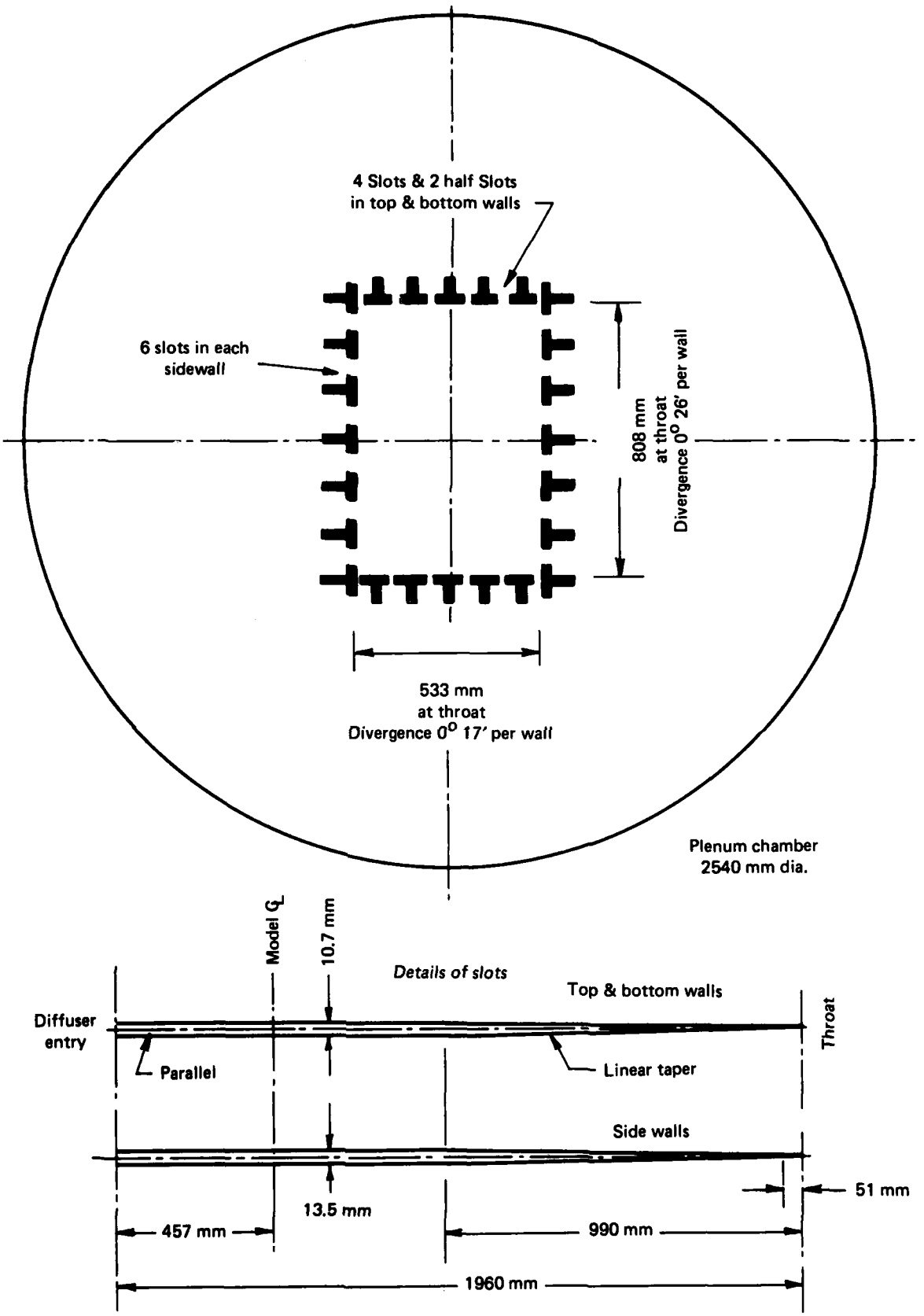

FIG 2. DETAILS OF SLOTTED TEST SECTION

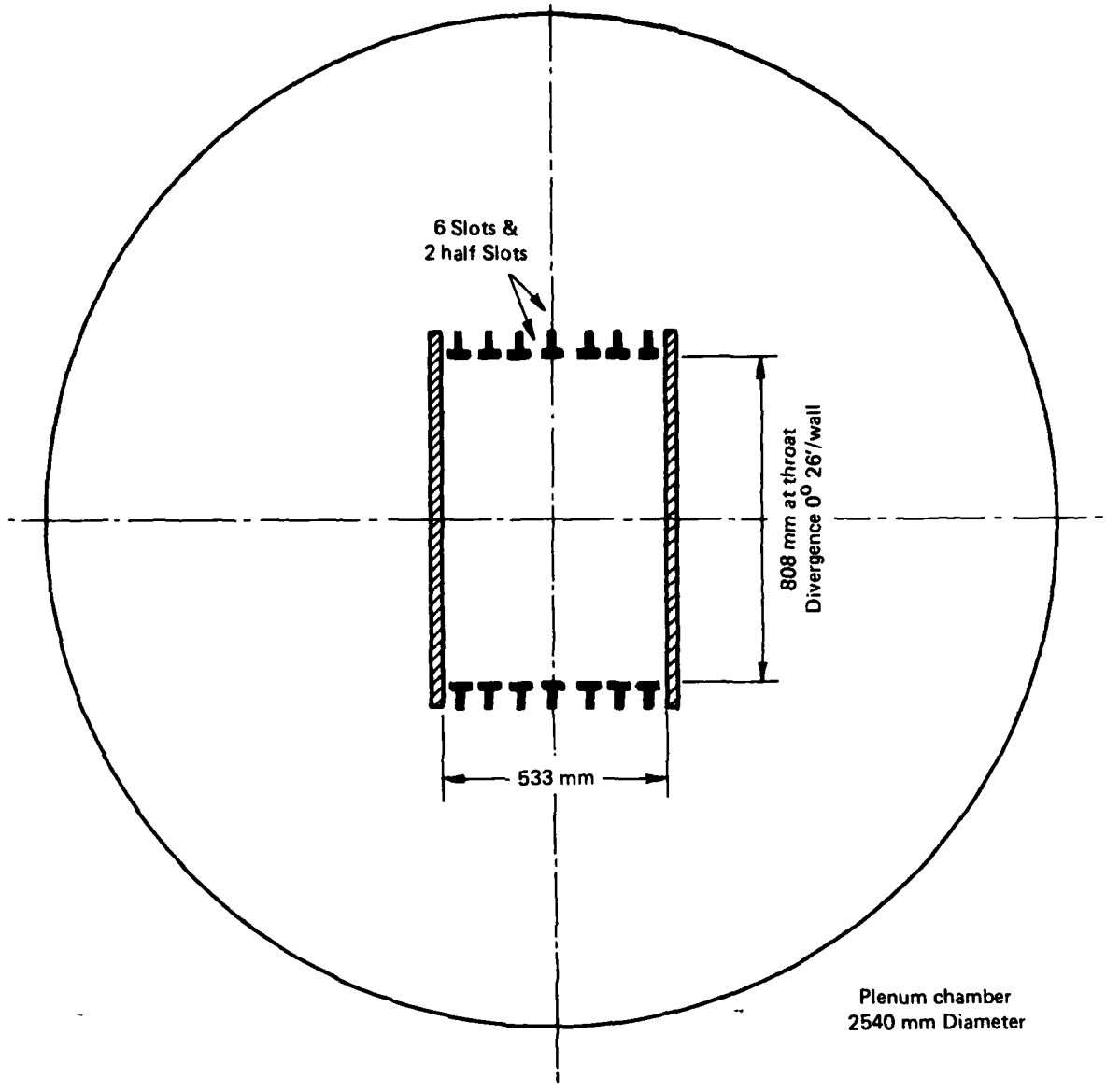

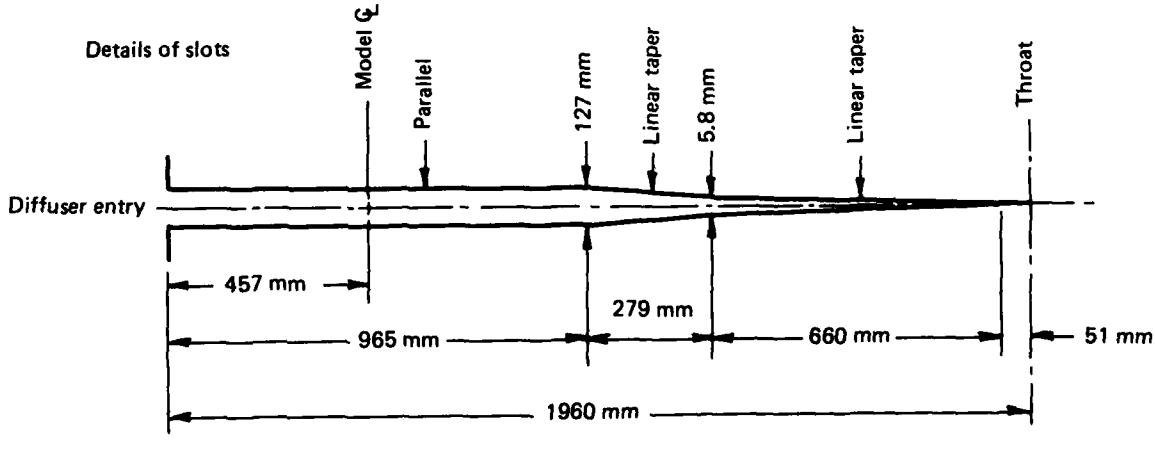

FIG 3. DETAILS OF SLOTTED WORKING SECTION

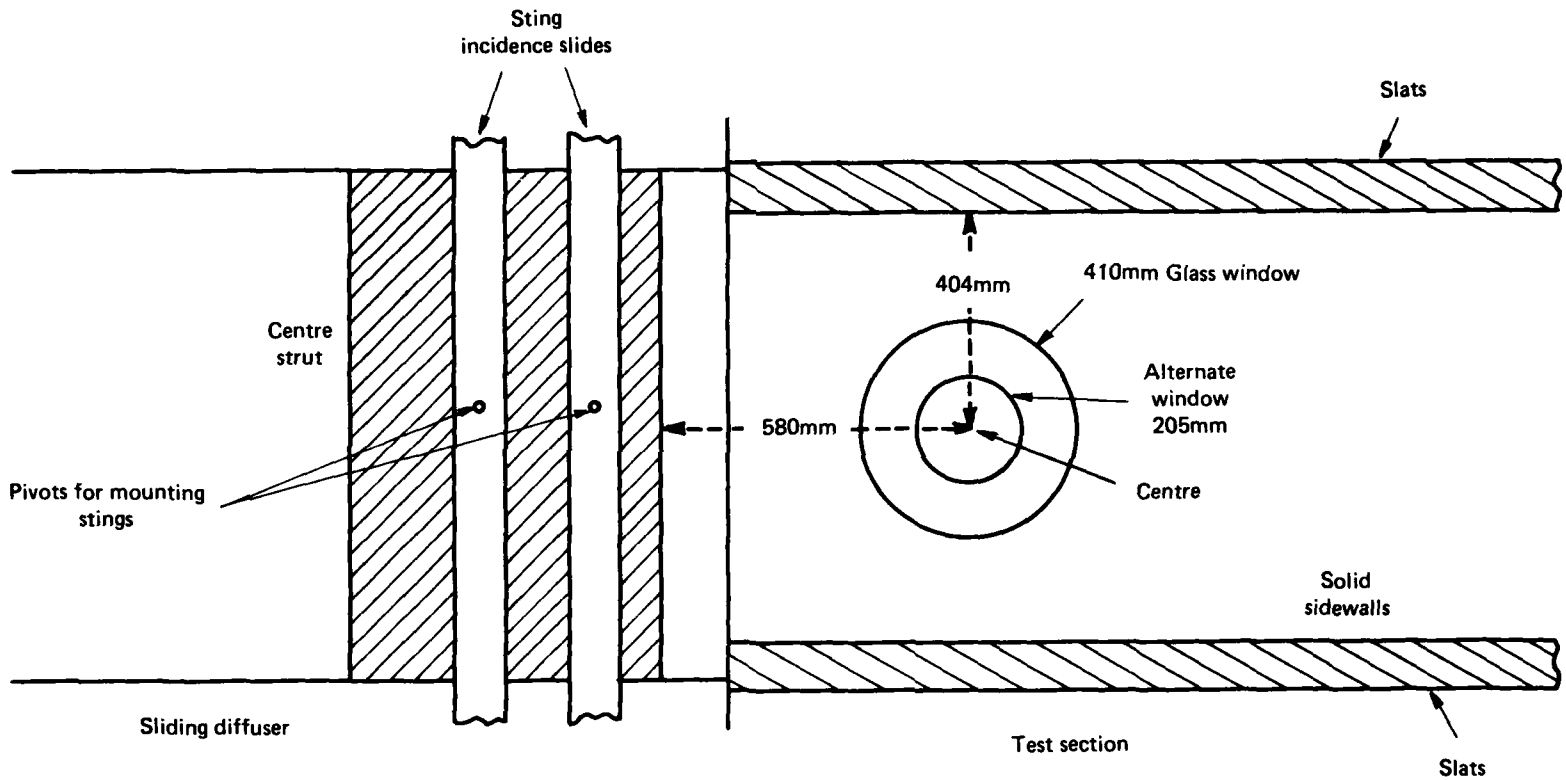

FIG 4. DETAILS OF STING SUPPORT STRUT AND SOLID SIDEWALLS WITH WINDOWS

a powered model can be made to "hover" in the test section but this becomes more and more difficult as the Mach number, and hence thrust required, rises. At transonic and supersonic speeds small models can be fired upstream so they pass through a test region before slowing down and dropping back through the test section again. The period of time in which the model can be observed depends on the test section length and the ratio of model mass to drag. It is however obvious that for the same test section length, the run time is much longer than for a ballistic range.

The first problems are how to fire what is probably a delicate model at the required speed and then how to catch it. While the firing could be explosive, it usually involves a piston, driven either by compressed air or a spring, from which a sabot-constrained model is released. (19) Recapture of the model is not necessary in a blow-down tunnel but in a closed circuit tunnel usually involves a net or screen. In the ARL transonic wind tunnel, the tunnel first diffuser angle is low and tunnel air-speeds between the test section and the compressor are high (up to $M_0 = 0{\cdot}7$) making model recapture without destroying the model virtually impossible.

The second problem is the conflict of model mass and moment of inertia requirements. The need to have model mass high to lengthen flight times has already been mentioned. The model moment of inertia, on the other hand, must be low to increase the rate of model response thus allowing study of more cycles of model oscillation in the same time. This is the reason such models (19) usually consist of a plastic or foam body with a heavy metal core.

Both the problem of recapture and the mass/moment of inertia conflict can be reduced if the model can be constrained in the x direction; i.e. along the tunnel centre line.

3.2 Models with No Freedom Along the Tunnel Axis

There are three main ways to restrain a model in x without seriously inpeding the other five spatial degrees of freedom; magnetic suspension, a towing line or a gimbal-type sting support. Some constraint in the other translational (y, z) modes is usually inherent in any such system but is not necessarily undesirable. Some systems further restrict the model to two degrees of freedom only.

3.2.1 Magnetic suspensions

With a magnetic suspension the model contains either permanent magnets or "soft" magnetic material and is suspended in a magnetic field either *with a field strength gradient* steep enough to maintain it in position against the drag force or variable by position sensing.

A passive system with a magnetic field shaped to hold the model towards the centre of the tunnel and at a fixed x-position requires a field concentration at the desired point. Such a concentrated field requires the magnetic poles to be much larger than the gap. The author has found no evidence that such a system has been successfully used.

An active system using electromagnets usually employs an optical means of position sensing. The sensing may be by means of separate light beams and photo-cells or may utilise photo-diodes or photo-transistors in the image plane of a schlieren or shadowgraph system. For a full 6-degree of freedom suspension, two such systems will be needed. A new optical system developed by O.N.E.R.A. (61) uses a scanning of a photo cathode image of a target on the model to detect movement; three such photomultiplier image detectors are needed for a 6-component system. The "V" system (10) shown in Figure 5, relies on model weight to balance the two sets of electromagnets. A drag solenoid overcomes x-axial movement. Such a system increases greatly in size and power requirements as tunnel size is increased. It is usually only used for small (under 200 millimetre diameter) low-density tunnels. The arrangement shown in Figure 5 for the ARL Transonic Tunnel would have a pole to model distance of 530 millimetres. The largest models used in this tunnel seldom exceed 410 millimetres in length and may be as short as 230 millimetres. The high ratio of pole gap to pole separation would make the normal "U" or horse-shoe shaped electromagnet very inefficient. In general, it would seem that the separation between the poles of these magnets should exceed the model to magnet distance.

Super conducting magnets have been suggested for such systems. They are unlikely to be used except for cryogenic tunnels and then probably only in intermittent flow tunnels.

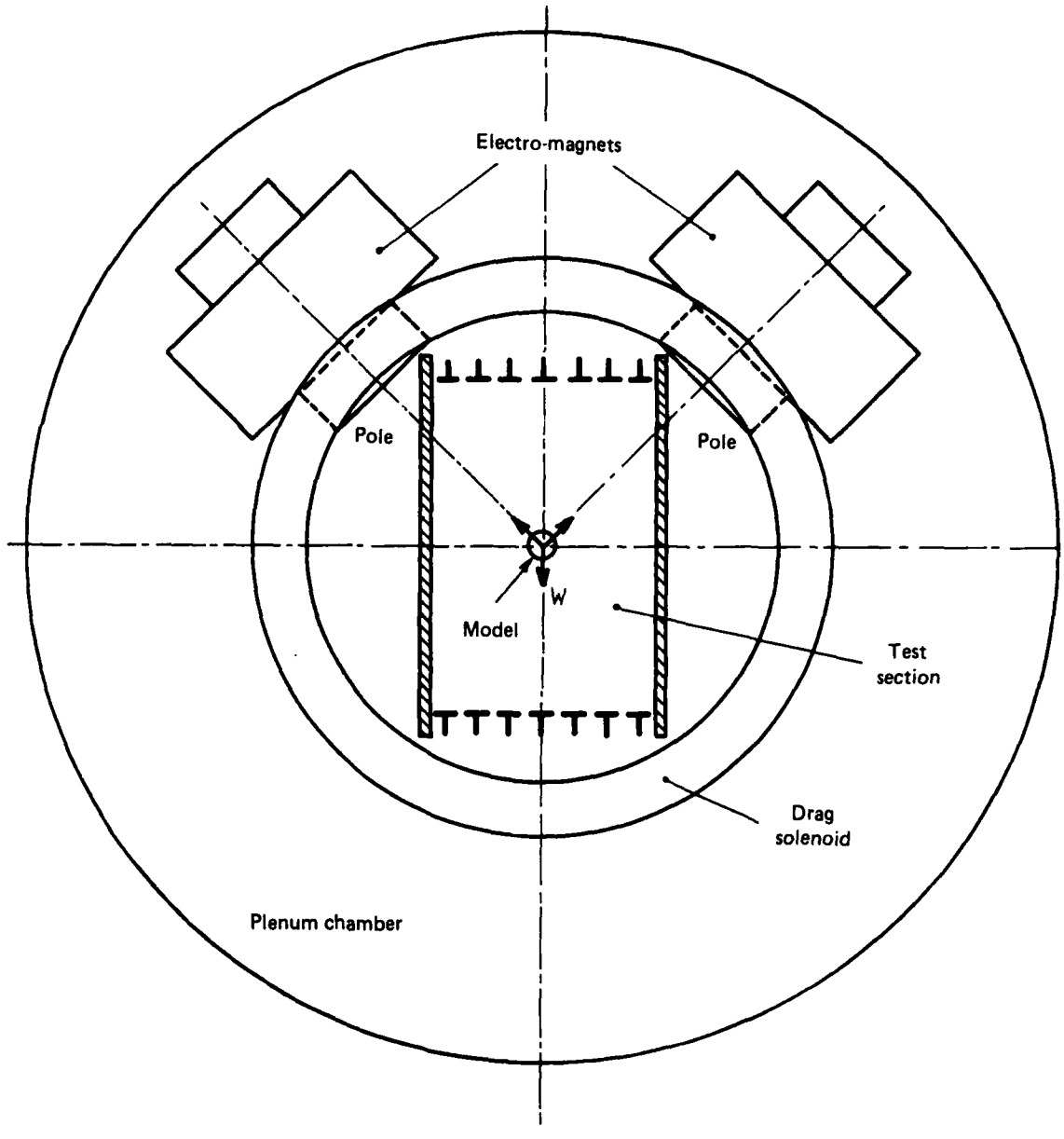

FIG 5. LAYOUT OF ELCTROMAGNETS REQUIRED FOR A MAGENTIC SUSPENSION IN TH
ARL TRANSONIC TUNNEL; POSITION SENSORS NOT SHOWN. (NOT PROPOSED)

3.2.2 Towed models

Towed models fall into two classes: passive models on a short towline whose restoring force to the centre of the tunnel is generated by the towline angle and active models on very long towlines using control deflections or gas discharges for positioning. In either case, the towline support is usually upstream of the contraction in a transonic or supersonic wind tunnel. Figure 6 shows the possible arrangement of an active model in the ARL transonic tunnel. The long distance between the tunnel viewing window and contraction entry would require a cable over 4·6 metres long. For a passive model and probably for most active ones, the cable would have to be semi-rigid for most of its length, leaving only a small flexible region ahead of the model. An additional problem would be the build up in boundary layer on such a long cable.

3.2.3 Sting supports with more than one freedom

Sting supports usually suppress all translational degrees of freedom apart from that due to rotations about points remote from the centre of gravity. Figure 7(a) shows a simple model mounted on a spherical air bearing. The bearing set at the model's centre of gravity allows free rotation in roll and limited displacements in yaw and pitch. Such a bearing exhibits no stiffness and very little damping. Accordingly it can only be used for configurations stable in both yaw and pitch. Figure 7(b) shows a modification of this in which a set of crossed-flexure pivots in a gimbol-type arrangement replaces the air bearing. This system exhibits stiffness but retains low damping. The roll motion is now restricted but this can be overcome if required. It has the further advantage that each degree of freedom appears between different platforms allowing the use of strain gauges to measure each angle or velocity sensing of each angular velocity. Figure (7c) is a variation on Figure 7(a) which requires no air supply. The spherical air bearing is replaced by a cone pivot with a conical point bearing on a conical depression of greater apex angle. A part-spherical retaining ring prevents the cones disengaging while the drag force normally maintains the clearance for the retaining ring.

Figure 7(d) shows an exception to the suppression of translational degrees of freedom. The model sting has spring pivots at two locations allowing two modes of oscillation. Provided the spring rates are chosen so that the natural frequencies of the two modes are quite different (the lower less than 40 percent of the higher) and the higher is not an integer multiple of the lower frequency, the two modes can be excited independently. If the two modes represent oscillations about centres respectively distances d1, and d2 behind the centre of gravity, then, assuming the Z force derivatives are small or known, the aerodynamic pitch-damping terms $C_{m\dot{\alpha}}$ and C_{mq} can be measurely independently. This arrangement has the further advantage that the pivot positions can be outside the model.

4. ALPHA, BETA MODES FOR MODELS WITH SINGLE DEGREES OF FREEDOM

Normal wind tunnel systems using constrained models allow the model to oscillate only in one possible mode. Two cases will be considered: one where the pivot centre coincides with the centre of gravity and the one where the pivot is offset along the x axis. Only the arrangement for pitch will be examined; yawing motions are similar but rotated 90 degrees. In each case, roll is suppressed.

4.1 The Un-restrained Free-oscillation Model

If the pivot coincides with the centre of gravity and is frictionless and provides no restraint in pitch, this represents the system called "pitching mode" in Reference 87.

Then
$$\alpha^1 \quad \theta \quad (\kappa/\omega)e^{\bar{\lambda}t}\sin(\omega t) \tag{4.1}$$

where
$$\bar{\lambda} \quad (C_{m\dot{\alpha}} + C_{mq})/2I_y \tag{4.2}$$

$$\bar{\omega}^2 \quad \bar{\omega}_0^2 - \bar{\lambda}^2 \tag{4.3}$$

and
$$\bar{\omega}_0^2 \quad - C_{m\alpha}/I_y \tag{4.4}$$

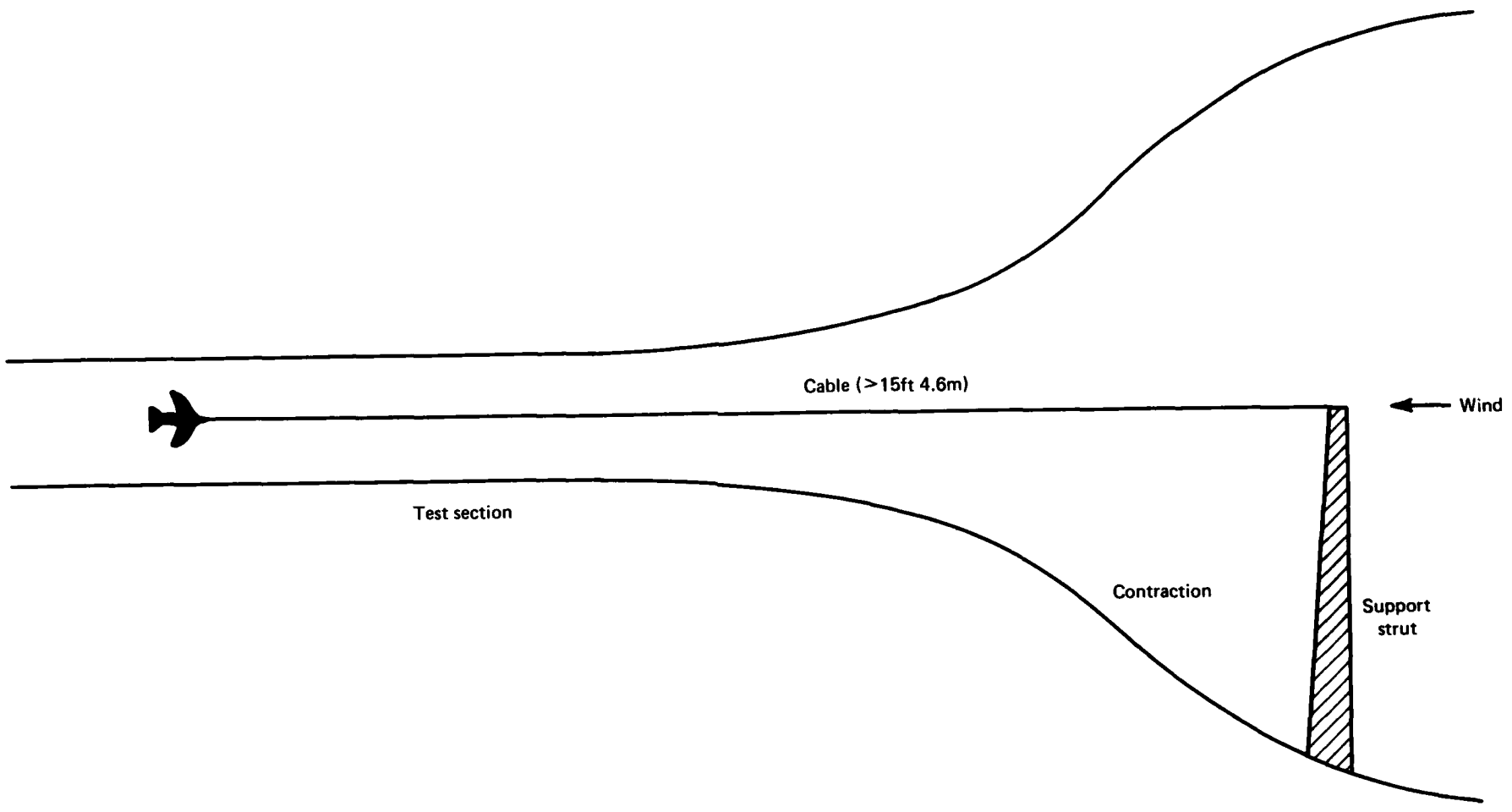

FIG 6. TOWED MODEL IN THE ARL TRANSONIC WIND TUNNEL (NOT PROPOSED)

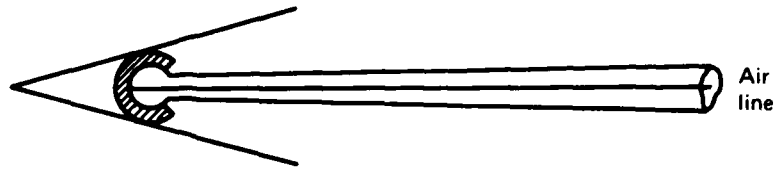

(a) Model on spherical air bearing

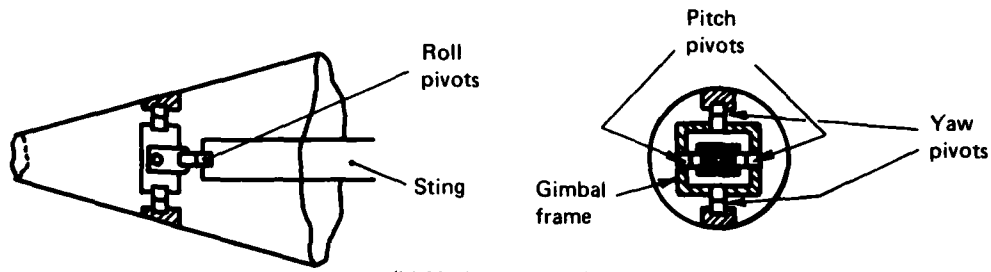

(b) Model on gimbal-type mounting.

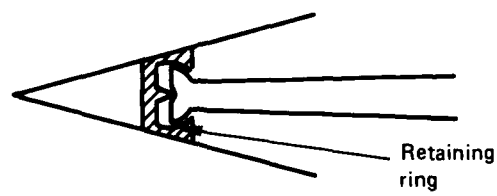

(c) Model on cone pivot.

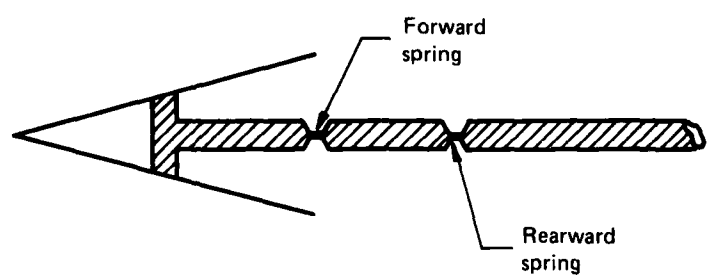

(d) Model with two pivot points.

FIG 7. MODELS WITH MORE THAN ONE ANGULAR FREEDOM

This gives a stable negatively-damped oscillation only if both C_{m_α} and $C_{m_{\dot\alpha}}$ are negative. Also, this implies (87) the additional requirements that reduced frequency $\bar\omega$ should be reproduced, and Mach number and Reynolds number correct. V_e is thus fixed while I_0 is usually smaller for the wind tunnel model. This necessitates a higher ω and means that I_y must also be accurately reproduced.

4.2 The Spring-Restrained Free-Oscillation Model

To overcome the limitation that I_y must be reproduced in the wind tunnel, a spring restraint system is added. If the centre of rotation is the body axes origin, then (87)

$$C_{m_{\dot\alpha}} + C_{m_q} = 2(\bar\lambda - \bar\lambda_t)I_y \tag{4.5}$$

and if

$$\bar\omega_{0_t}{}^2 = \bar\omega_t{}^2 + \bar\lambda_t{}^2 \tag{4.6}$$

is the frequency of the tare (wind-off) system,

and

$$\bar\omega_0{}^2 = \bar\omega^2 + \bar\lambda^2 \tag{4.7}$$

is the frequency with wind-on, then

$$C_{m_\alpha} = (\bar\omega_0{}^2 - \bar\omega_{0_t}{}^2)I_y \tag{4.8}$$

In most cases the spring constant K_θ is known and the tare values thus determine I_y.

Provided the model is oscillated about an axis displaced $-x_0$ along the x axis, then the α and q derivatives are no longer coupled as in equation 4.5, but still can not be found independently since

$$(C_{m_\alpha} + \bar x_0 C_{z_\alpha}) = -(\bar\omega_0{}^2 - \bar\omega_{0_t}{}^2)I_{y_1} - \bar\omega_0{}^2\bar x_0(C_{m_{\dot\alpha}} + \bar x_0 C_{z_{\dot\alpha}}) \tag{4.9}$$

and

$$(C_{m_{\dot\alpha}} + \bar x_0 C_{z_{\dot\alpha}})(1 + \bar x_0{}^2\bar\omega_0{}^2 - 2\bar\lambda\bar x_0) + (C_{m_q} + \bar x_0 C_{z_q}) = [2(\bar\lambda - \bar\lambda_t) - \bar x_0(\bar\omega_0{}^2 - \bar\omega_{0t}{}^2)]I_{y_1} \tag{4.10}$$

give only two equations in six unknowns. I_{y1} is the normalized moment of inertia about the new axis and, as before, can be measured from the tare values if the spring constant is known. In fact, this method of determining I_y is used even for full-sized aeroplanes (64).

The six derivatives (C_{m_α}, $C_{m_{\dot\alpha}}$, C_{m_q}, C_{z_α}, $C_{z_{\dot\alpha}}$, C_{z_q}) can be determined if three values of x_0 are used. However, the accuracy of the force derivatives and the separation between C_{m_q} and $C_{m_{\dot\alpha}}$ depends on $\bar x_0$. The accuracy of C_{m_α} and $C_{m_{\dot\alpha}} + C_{m_q}$ depends on the accuracy of measuring ω and λ.

In this case of spring restraint then, the accurate reproduction of ω is accomplished using the spring constant and I_y need not be accurately reproduced. However, I_y for the model should still be as low as possible to reduce loadings.

4.3 The Spring—Restrained Forced Model

Free systems have been considered about two axes, one corresponding to the moment centre and one offset in the $-x_0$ direction. Each of these will now be discussed with an external torque added. Section 6 of Reference 87 solves the equations about the y_0 axis. Again the mechanical parameters are given by a tare case and a similar form of motion exists for wind on or off.

Provided the system is stable at its natural frequency (ω_0) the motion after the initial transient is of the form,

$$\theta = \theta_1 e^{j(\Omega t + \xi)} \tag{4.11}$$

where

$$\xi = \tan^{-1}[2\bar k\bar\Omega/(\bar\omega_0{}^2 - \bar\Omega^2)] \tag{4.12}$$

and

$$\theta_1 = T_0/[I_y\{4\bar k^2\bar\Omega^2 + (\bar\Omega^2 - \bar\omega_0{}^2)^2\}^{\frac{1}{2}}] \tag{4.13}$$

and where the impressed torque is $T_0 e^{j\Omega t}$

These equations simplify under particular conditions. For a resonance condition, i.e.

$$\Omega^2 = \omega_0{}^2 \tag{4.14}$$

then $$\xi = 90^\circ \text{ (quadrature)} \tag{4.15}$$

and $$\theta_1 = T_0/(2I_y k\bar{\Omega}) \tag{4.16}$$

If $\bar{\Omega}$ is much smaller than $\bar{\omega}_0$ and (4.12) is expressed in terms of a frequency ratio

$$\eta = \Omega/\omega$$

and angular damping index $\kappa = \lambda/\omega$

then $$\tan \xi = 2\kappa\eta/(1 + \kappa^2 - \eta^2)$$

and for small η and κ,

$$\xi \approx 2\kappa\eta$$

For an axis of rotation displaced $-x_0$, Section 4.2 gives the unforced system. The forced system will give this solution as a transient but for $\omega \neq \Omega$ the output after a finite time will again be

$$\theta = \theta_1 e^{j(\Omega t + \xi)} \tag{4.17}$$

if the applied torque is $T_0 e^{j\Omega t}$.

As before, $$\xi = \tan^{-1}(2\bar{\lambda}\bar{\Omega}/(\bar{\omega}_0^2 - \bar{\Omega}^2)) \tag{4.18}$$

and $$\theta_1 = T_0/[I_y\{4\bar{\lambda}^2\bar{\Omega}^2 + (\bar{\Omega}^2 - \bar{\omega}_0^2)^2\}^{\frac{1}{2}}] \tag{4.19}$$

but the quantities ω_0 and λ are now given by (4.9) and (4.10), and the same comments as before apply.

In each of these forced cases, the required reduced frequency is impressed upon the system and neither I_y nor $\bar{\omega}_0$ need be accurately reproduced. The value of θ_1/T_0 is called the magnification factor and for zero damping is equal to

$$1/\{\bar{\omega}_0^2 I_y(1 - \eta^2)\}$$

where

$$\eta = \Omega/\omega_0$$

is the frequency ratio. When $\eta = 1$, this implies a resonance condition and θ_1 increases linearly with time (zero damping).

In each of these cases, the free system does not have to be stable since the damping necessary to reduce the free system to a transient response can be imposed mechanically.

4.4 The Rigidly-Driven Model

It the model were rigidly driven at constant amplitude, constant frequency, no transients occur and no moments of inertia have to be matched. However, it is now impossible to obtain information about the model from its motion. Forces and moments have to be measured. For a pitch oscillation, the normal force Z and pitching moment m have the coefficient form

$$C_z = C_{z_0} + C_{z_\alpha}\alpha + C_{z_{\dot{\alpha}}}\dot{\bar{\alpha}} + C_{z_q}\dot{\bar{\theta}} \tag{4.20}$$

and

$$C_m = C_{m_0} + C_{m_\alpha}\alpha + C_{m_{\dot{\alpha}}}\dot{\bar{\alpha}} + C_{m_q}\dot{\bar{\theta}} \tag{4.21}$$

respectively.

The motion is given by

$$\theta = \alpha = \theta_0 + \theta_1 e^{j\Omega t} \tag{4.22}$$

and equations 4.20 and 4.21 represent components $\theta_1 C_{z_\alpha}$ for C_z and $\theta_1 C_{m_\alpha}$ for C_m in phase with the motion and components $\Omega\theta_1(C_{z_{\dot{\alpha}}} + C_{z_q})$ and $\Omega\theta_1(C_{m_{\dot{\alpha}}} + C_{m_q})$ in quadrature. All forces and moments measured thus have to be resolved into components in phase and in quadrature with the motion.

Since any strain gauge balance used to measure these forces and moments represents a

spring, however stiff, between the forcing unit and the model, balance stiffness and natural frequency are critical terms in this method.

4.5 The Model Driven Through a Spring

If a spring were inserted between the model and the rigid drive unit, a system would be obtained with an amplitude depending upon the aerodynamic conditions. The situation is similar to that of Section 4.3 but with applied torque

$$Q_\theta(T_0 e^{j\Omega t} - \theta) \tag{4.23}$$

and not $T_0 e^{j\Omega t}$ as before, and where Q_θ is the spring constant of the spring inserted. The same transients as before would appear but with tare value ω_t depending on the overall spring constant $K_\theta + Q_\theta$ and not just K_θ.

For the impressed motion

$$\theta = \theta_1 e^{j(\Omega t - \xi)} \tag{4.24}$$

where

$$\xi = \tan^{-1}(2\bar{\lambda}\bar{\Omega}/(\bar{\omega}_0^2 - \bar{\Omega}^2)) \tag{4.25}$$

and

$$\theta_1 = Q_\theta T_0/[I_y\{4\bar{\lambda}^2\bar{\Omega}^2 + (\bar{\Omega}^2 - \bar{\omega}_0^2)^2\}^{\frac{1}{2}}] \tag{4.26}$$

where the note above about ω depending on $K_\theta + Q_\theta$ still applies.

The situation is thus dynamically identical with that in Section 4.3.

4.6 The Curved Model

Most of the tunnel methods considered so far have measured the combined pitch damping term $C_{m\dot{\alpha}} + C_{mq}$. These terms can be separated using curved models on static balances (11).

FIG. 7(e) CURVED CONE MODEL DURING MANUFACTURE AT ARL

In this case the apparent pitch angle of the model varies along its length, usually as a circular arc. This situation may be interpreted (88) by considering an aircraft flying, at constant incidence, a circular arc in the pitch plane. As α is constant, $\dot{\alpha}$ is zero and $\dot{\theta} = q$ is a constant. The flow is curved on a circular arc; by change of co-ordinates (conformal mapping) this situation can be converted to parallel flow over a curved model.

If the radius of curvature of the model is R, then the difference in pitch over the reference length is

$$\Delta\theta = l_0/R \tag{4.27}$$

A time $\Delta t = l_0/V_e$ is associated with this length and leads to

$$q = \Delta\theta/\Delta t = V_e/R \tag{4.28}$$

In Aero-Normal terms,

$$\bar{q} = 1/\bar{R} \tag{4.29}$$

and the expression for the measured pitching moment is:

$$C_m = C_{m_0} + C_{m_\alpha}\alpha + C_{m_q}/\bar{R} \tag{4.30}$$

This method requires only a static balance but needs at least two models and does not measure $\dot{\alpha}$ derivatives.

5. METHODS FOR OSCILLATION OF STING-MOUNTED MODELS

Three separate sub-systems make up any dynamic test rig; the model pivot, the measurement of model response and the displacing or forcing mechanism. These will be considered in turn for each type of rig investigated but a more-general look at pivots will be made first.

For a single angular degree-of-freedom system there must exist a fixed pivot point either real or virtual. Figure 8 illustrates some of the pivot types for a sting-mounted model with a real pivot point. These are divided into two types, where the pivot point is either internal to the tunnel or external. Cases where the pivot is internal to the tunnel are shown in Figures 8(a), (b), (c) and (d) and it should be noted that these pivots are largely internal to the model also. They include air-bearings Figure 8(a), flexural pivots and crossed flexures Figure 8(b), twin cone pivots Figure 8(c), single spring pivots Figure 8(d) and, of course, ball, roller and needle roller bearing assemblies. Systems with pivots external to the tunnel are shown in Figure 8(e) and are mechanically identical to systems with models mounted on the side windows and will be included with them in the next section (6).

Three examples of virtual pivot centres are shown in Figure 9. These are useful if a pivot will not fit at the required point e.g. if the desired centre of oscillation is ahead of the model or in a restricted part of the model. They represent more complicated and less rigid pivots than the real-centre pivots of Figure 8. Also the twin-link four-pivot system of Figure 9(b) is suitable for only small angular deflections as the pivot point moves with displacement. For certain methods of displacement one of the connecting links in this system may be replaced by part of the driving mechanism. The actual pivots involved in a virtual-centre system are of the same types as used in the real-centre cases.

The choice of pivot will depend on the model, the axis required and the method of oscillation chosen.

5.1 Free Oscillation with Internal Pivot

Currently in use in the ARL Transonic Tunnel is a free oscillation dynamic rig based on that designed by the Sandia Corporation (20). At present, the pivot consists of two miniature ball-bearing races, and spring constraint and a strain-gauge displacement signal are provided by a thin offset beam (Fig. 10). Current difficulties with the locally built rig include a non-sinusoidal motion due to irregular bearing friction and a non-sinusoidal output due to play in the link between the head and torque beam. The use of flexural pivots (Fig. 11) instead of bearings, and of tighter machining tolerances on other parts is being investigated in an effort to overcome these deficiencies.

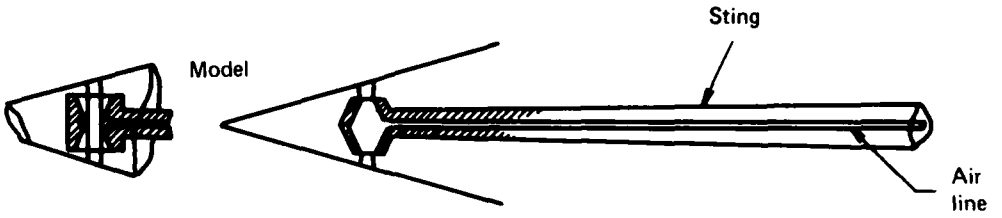

(a) Model with double-tapered air bearing (two forms).

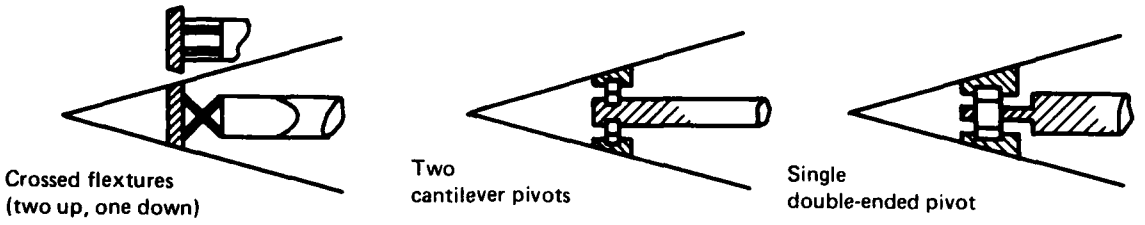

(b) Model on flexural pivots or cross flextures.

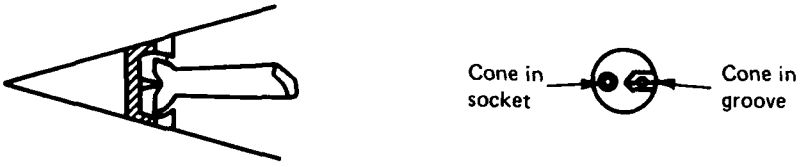

(c) Model on twin core pivots.

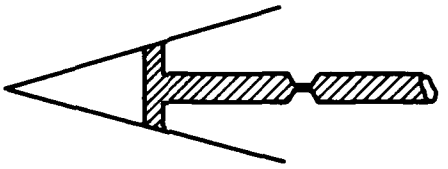

(d) Model on single spring.

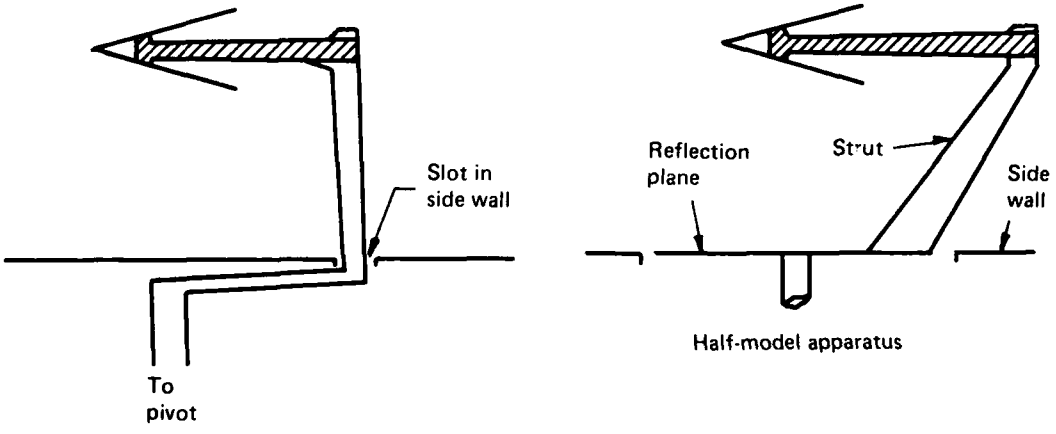

(e) Model with pivots external to tunnel (two forms).

FIG 8. MODELS WITH ONLY ONE (ANGULAR) DEGREE OF FREEDOM

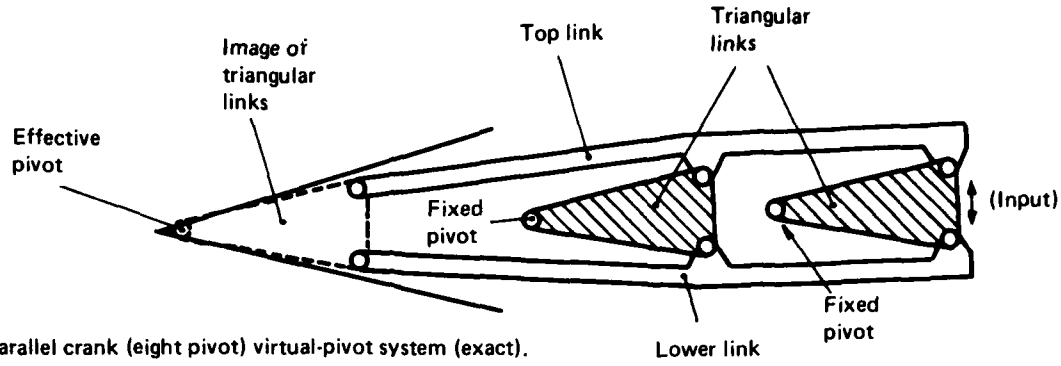

(a) Parallel crank (eight pivot) virtual-pivot system (exact).

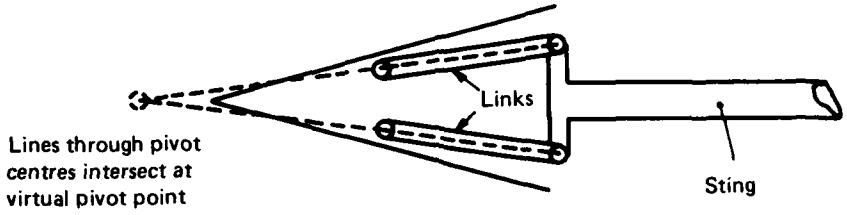

(b) Four pivot virtual-pivot system (Approximate).

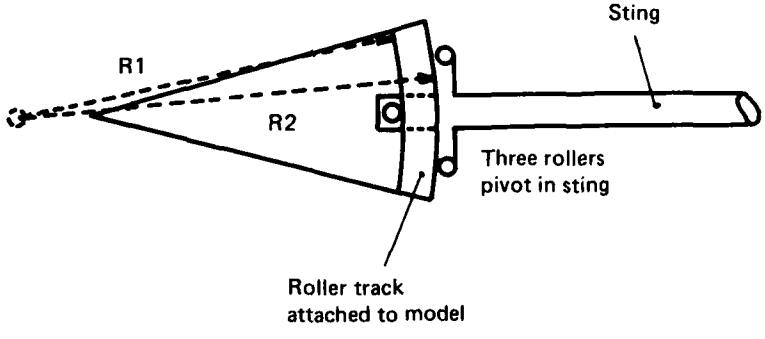

(c) Three roller virtual-pivot system (exact).

FIG 9. EXAMPLES OF VIRTUAL PIVOT CENTRES SHOWING LOCATION OUTSIDE MODEL

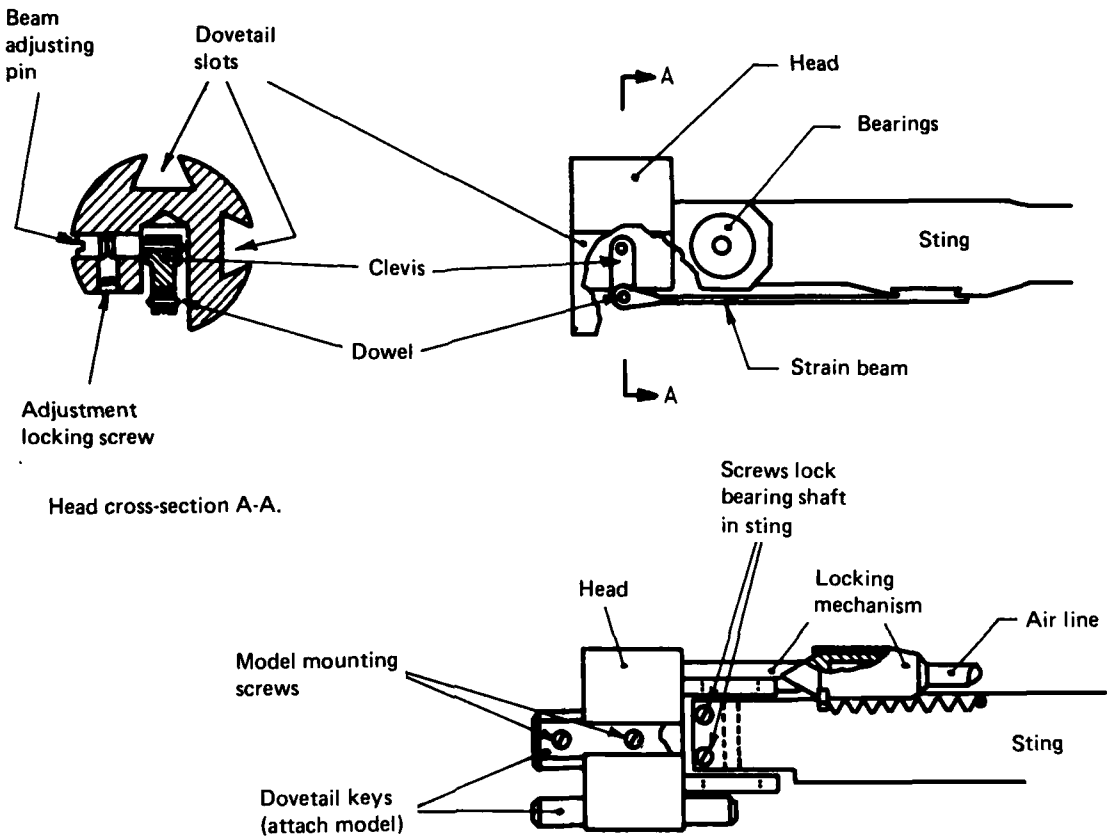

FIG 10. SIMPLIFIED VIEW OF CURRENT SANDIA-TYPE FREE-OSCILLATION RIG (DEFLECTION MECHANISM NOT SHOWN)

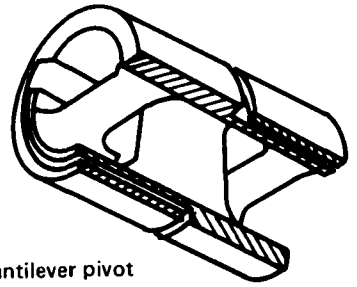

Cantilever pivot

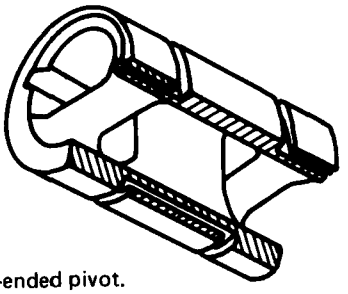

Double-ended pivot.

FIG 11. FLEXURAL PIVOTS: PART SECTION VIEWS OF TWO TYPES

Other pivots which have been used, particularly by AEDC-VKF, include (10) machined cross-flexures, cruciform and Torque-Tube pivots. In each of these cases, a new pivot is needed for every change in stiffness required. Also both the torque tube and cruciform shape would appear difficult to machine in the size required at A.R.L. Strain-gauging these to produce a displacement output could also present some problems. The cross-flexures (Fig. 12) on the other hand are comparatively easy to machine in the multipiece construction used by AEDC-VKF, and strain-gauging of the flexures is straight-forward. The assembly of this pivot, as with those already in use at A.R.L., must be free of movement to preclude hysteresis.

The pivot design most suitable would appear to be that shown in Figure 13 with commercially available flexural pivots providing location and a single replacable strain-gauged beam to provide both displacement output and variation in stiffness. For higher loads than the flexural pivots can carry, the AEDC-VKF-type crossed flexures should be used.

The second requirement for a free-oscillation rig is a means of measuring model response. Since the motion is periodic, it is characterized by either its displacement, velocity or acceleration. Figure 14 shows methods suitable for both free and forced rigs. It is considered that the measurement made should be of displacement to permit direct monitoring of the model position with respect to the rig limits. The type of displacement sensor would be chosen from those in Figure 14(c) depending on the choice of pivot. The final design will be determined by the space available and the required accuracy of measurement. Figure 15 compares the configurations of Figure 14(c). Configurations (ii), (iii) and (v) have moment-type bending of the strain-gauge beam with various amounts of axial (tension) loading. The other two configurations are not uniformly stressed, they have force-type bending. However the major difficulty with these is the effect of stiffness in the pin-jointing.

The arrangement of Figure 13 is an inversion of the configuration (i) of Figures 14(c) and 15. The sign of the second order term will now be positive. For the dimensions shown in Figure 13 this arrangement has a non-linearity of approximately $0{\cdot}5\%$ at 3 degree deflection provided the link pivots exert little torque. The arrangement of Figure 10 is configuration (iv) of Figures 14(c) and 15. Here the non-linearity due to the tilt of the connecting link is negligible.

The other requirement of a free-oscillatory system is a means of model displacement. The SANDIA-type rig shown (20) in Figure 16 has a mechanism in a sting-flare operating a lever inside the model. This system has the advantage of having no bulky mechanism inside the model itself. Other methods which have been used include air jets impinging on the inside of the model.

Each of the rigs discussed under this section (5.1) represent the spring-restrained free-oscillation model of Section 4.2. Instrumentation for this technique will be discussed in another Note of this series.

5.2 Forced Oscillation about an Internal Pivot

The requirements for pivots and displacement sensing in this case are the same as for the free-oscillation case of 5·1, but the displacing mechanism now becomes a forcing mechanism. Two classes of forcing mechanism exist: those applying a torque to the model equivalent to the system of Section 4.3, and those where a rigid drive connects to the model via a spring as in Section 4.5.

The latter method has the defect of lack of control over test conditions: without changing the spring-rate or the amplitude of the rigid drive only frequency is easily changed. The applied-torque method on the other hand is extremely flexible. A step pulse in torque followed by a steady or zero torque simulates free-oscillation techniques while a feed-back loop can maintain a constant amplitude oscillation simulating a rigid drive but with the advantage of a known torque input.

The applied torque can be applied directly by a rotary drive such as a D.C. electric motor fed with A.C. at the required frequency. As long as the motor response is linear, this will produce an oscillatory torque at the motor shaft. However, it is often difficult to position the motor at the axis of rotation so a long drive shaft may be necessary, as well as a means of changing the direction of the axis of rotation. It generally proves less trouble to use a linear force-producing unit such as an electromagnetic or hydraulic shaker. The long shaft now moves back and forth, not rotates. To convert this motion to rotation, this shaft may connect to the model away from the axis of rotation. If the shaft and the line through this connection to the pivot form a right

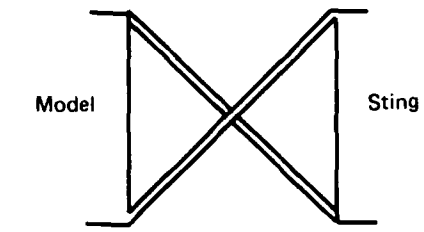

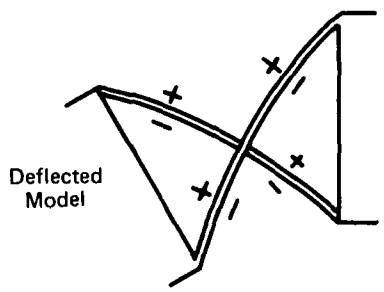

Deflection bends strips into circular arcs

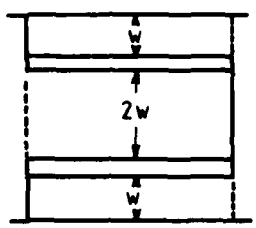

Centre strip twice width outer pair or use two pair

FIG 12. CROSSED FLEXURES: SOME FEATURES OF THIS TYPE OF PIVOT

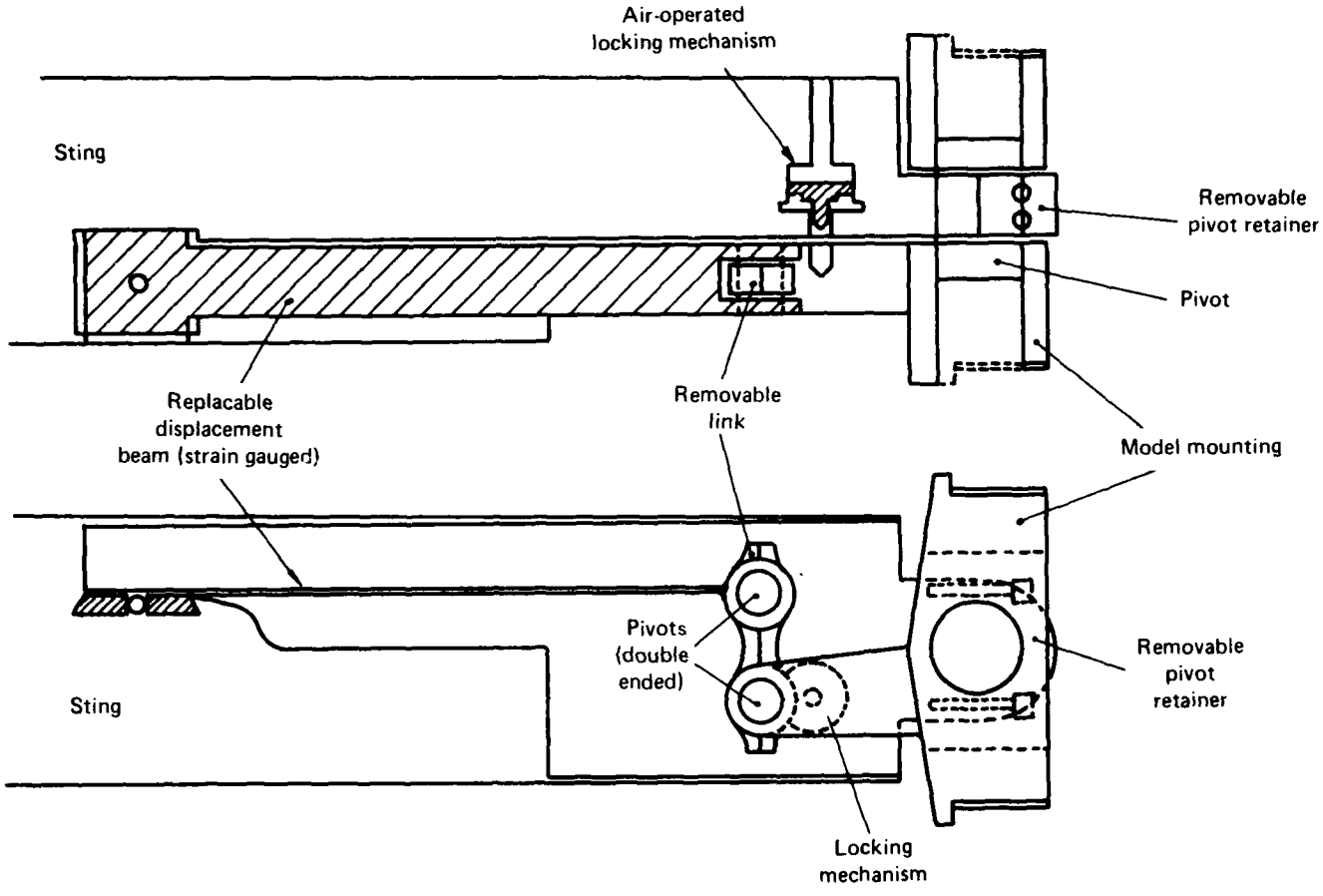

FIG 13. DESIGN OF FREE-OSCILLATION STING BALANCE TO SUIT ARL TRANSONIC TUNNEL
(TWICE FULL SIZE)

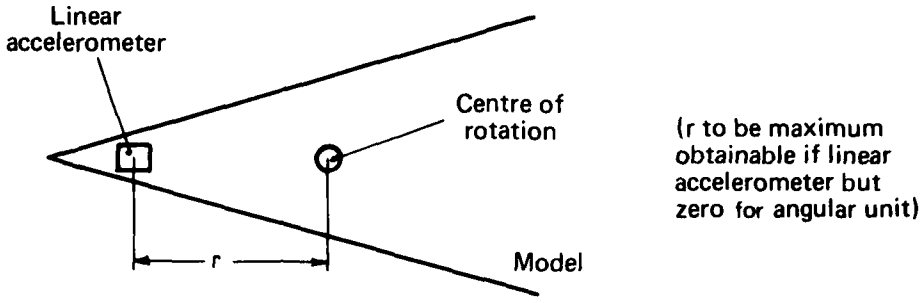

(a) Measurement of acceleration

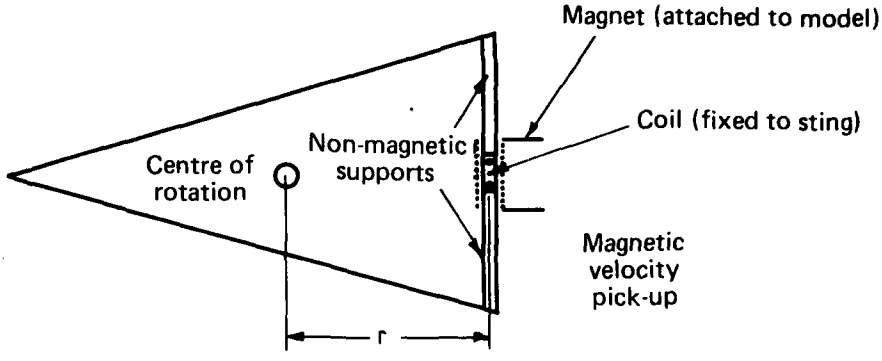

(b) Measurement of velocity

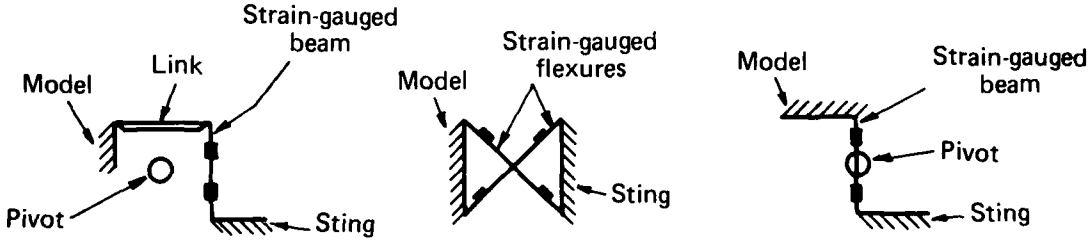

(i) Parralelogram linkage (ii) Crossed-flexures pivot (iii) Interconnecting beam

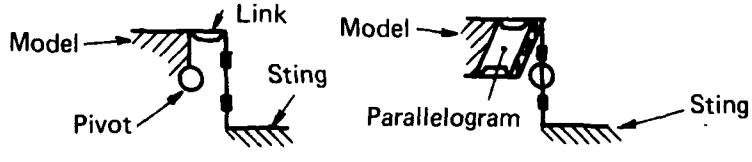

(iv) Variation on (i) (v) Modification of (iii)

(c) Measurement of displacement using strain gauges

FIG 14. PROVISION OF A POSITION SIGNAL FOR FREE OR FORCED DYNAMIC RIGS

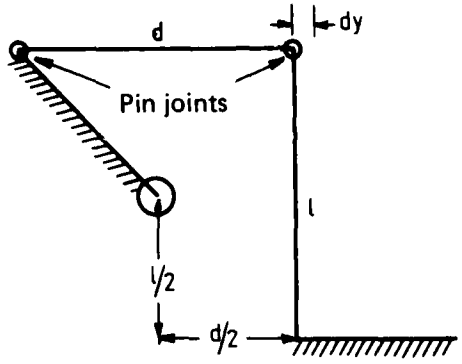

(i)

Force-Type bending
$dy \approx l/2\ \theta - d/8\ \theta^2$

(Any stiffness in pin joints gives tension and movement in beam proportional to θ/d)

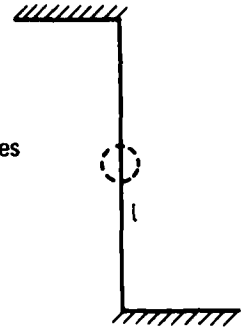

(ii) Crossed flexures
(iii) Separate pivot

Moment-Type bending
Beam curvature = $1/R = \theta/l$
Beam tension (ii) $\approx$ o
Beam tension (iii) strain = $\theta^2/24$

(v)

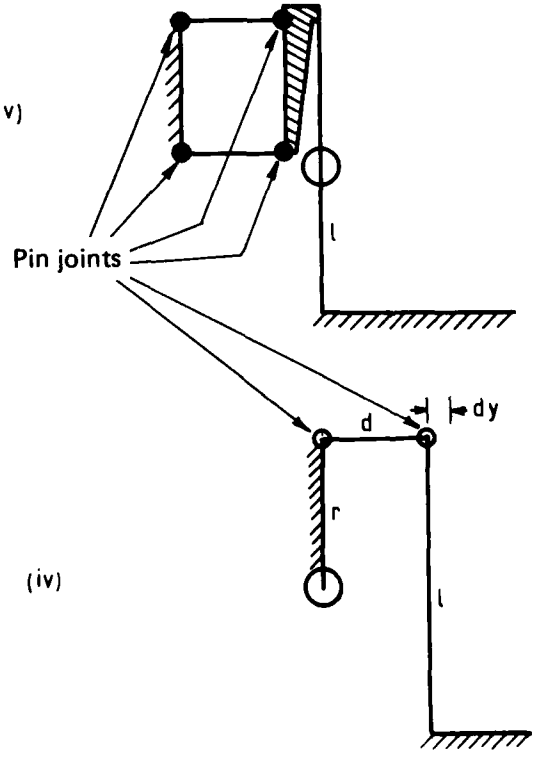

(iv)

Moment - Type bending
As for (ii) above
(Any stiffness in pin joints gives tension in beam)

Force – Type bending
$dy \approx r\ \theta$ for link horizontal
(l, d, r can be chosen to keep link close to being horizontal)
(Any stiffness in pin joints gives tension and moment in beam)

FIG 15. EFFECT OF A DEFLECTION θ BETWEEN MODEL AND STING FOR THE DISPLACEMENT BEAM CONFIGURATIONS OF FIG 14. (c)

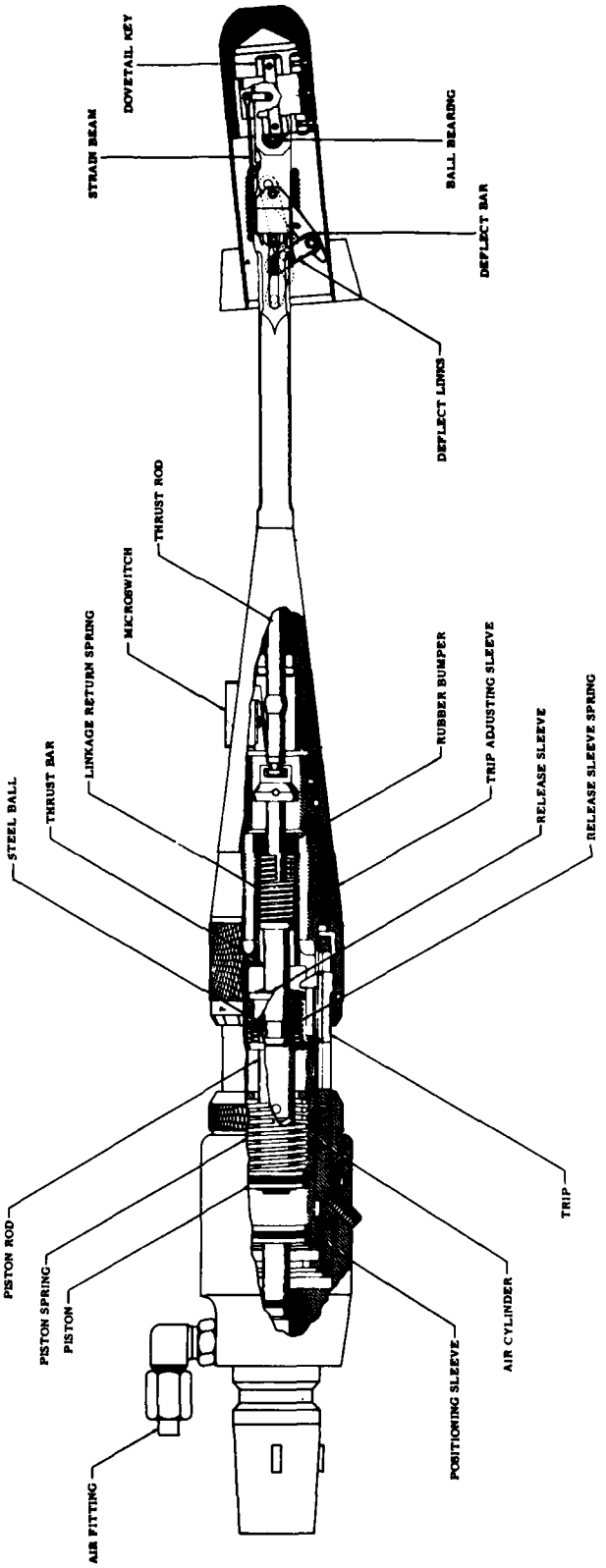
DOVETAIL KEY
STRAIN BEAM
BALL BEARING
DEFLECT BAR
DEFLECT LINKS
THRUST ROD
MICROSWITCH
LINKAGE RETURN SPRING
THRUST BAR
STEEL BALL
RUBBER BUMPER
TRIP ADJUSTING SLEEVE
RELEASE SLEEVE
RELEASE SLEEVE SPRING
PISTON ROD
PISTON SPRING
PISTON
AIR FITTING
POSITIONING SLEEVE
AIR CYLINDER
TRIP

FIG 16.

angle, then a linear harmonic motion of the shaft produces an angular harmonic motion of the model for some small angle of rotation. Unfortunately it also produces a lateral movement in the sliding shaft. Figure 17 shows two methods of absorbing this and returning the shaft to the centre-line as well. The Scott-Russell (triangular) mechanism is the simplest but imposes a greater restriction on tolerance at the sliding bearing than does the parallelogram linkage.

The parallelogram linkage has an additional advantage. Since bearings are between the forcing unit and the model, the torque applied should be measured between these bearings and the model. The upright arm of the parallelogram linkage is an excellent location for measuring the force applied to the connecting link and hence torque on the model.

To reduce power levels and simplify data reduction a forced dynamic rig may be operated at resonance. If a wide range of tests are required at resonance, it may be necessary for a variable spring rate to be included in the rig design. Figure 18 shows some of the methods for obtaining a variable spring rate.

Figure 19 is part of the general arrangement drawing of a forced rig being constructed for the ARL Transonic Wind Tunnel. It uses flexural pivots, the displacement beam system of Figure 14(c) (v) and Figure 15(v), a variation on the parallelogram torque linkage of Figure 17(b) and a tunable spring as per Figure 18(i). The model is forced by an electromagnetic shaker and a DC motor with position indicator moves the tuning spring back and forth to alter its effective length.

Instrumentation for this technique is discussed in a subsequent Note of this series.

5.3 Rigidly-imposed Oscillation about an Internal Pivot

The forcing mechanism of Section 5.2 now becomes a rigid drive. The mechanism required depends on the space available, pivot type and location and the amplitude of the oscillation. Figure 20 comprises two mechanisms suitable for larger amplitudes. If the swash plate inclination and bend in the bent shaft are of angle ψ then these produce a model angle

$$\theta = \psi \sin \phi \tag{5.1}$$

for an input shaft angle ϕ. These techniques require large model diameters and reasonably large amplitudes to be accurate. Techniques more suitable for smaller ψ are given in Figures 21 and 22. The skewed-space-linkage of Figure 21 involves a link which moves to describe the surface of a cone of half-angle ψ. The model is restrained to oscillate about a fixed axis and the link is allowed to oscillate in the model axis. The more common mechanism is the Scotch Yoke of Figure 22. The ball end of the crank describes the same path as for the skewed-space-linkage but the conversion to rotary-oscillatory motion is accomplished by the crank end sliding in a slot in the model arm. Since the radial distance from the model axis of rotation is greater, the allowable free-play in this slot is greater than the skewed-space-linkage, for the same accuracy of movement.

The choice of mechanism is influenced by the other requirements of a rigid-drive rig. Pivot and mechanical friction is no longer a problem, displacement can now be measured by the orientation of the input drive shaft and a balance is required to measure model loads. This balance must be situated between the driving unit and the model, and preferably between the model pivots and the model. Both the skewed-space-linkage and the Scotch Yoke offer space for such a balance, Figures 21 and 22, but the Scotch Yoke has the advantage of allowing the balance to measure moments about the axis of rotation directly. This greatly improves measurement accuracy and is the major reason for choosing the Scotch Yoke arrangement. For both mechanisms ψ is varied with a variable or interchangeable crank pin.

If the required centre of rotation were outside the model or in a restricted part of the model, a virtual pivot arrangement might have to be used. Figure 23 shows an exact virtual pivot Scotch Yoke mechanism and Figure 24 a simpler approximate method. If sufficient rigidity can not be obtained with a virtual pivot, results would have be obtained at two pivot locations and transposed to the required location.

Instrumentation for this method is discussed in a subsequent Note.

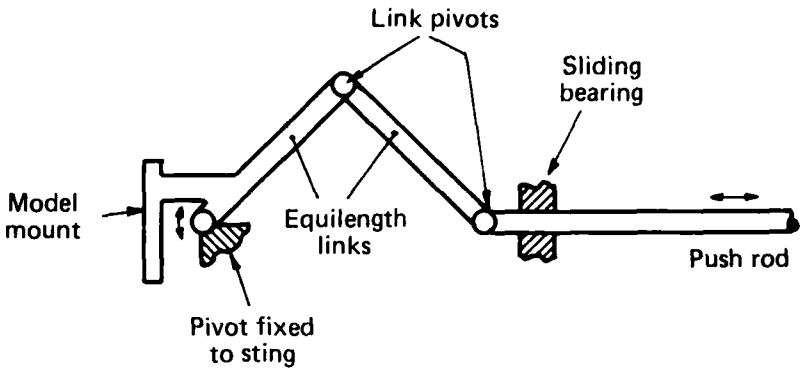

(a) Scott-Russell mechanism

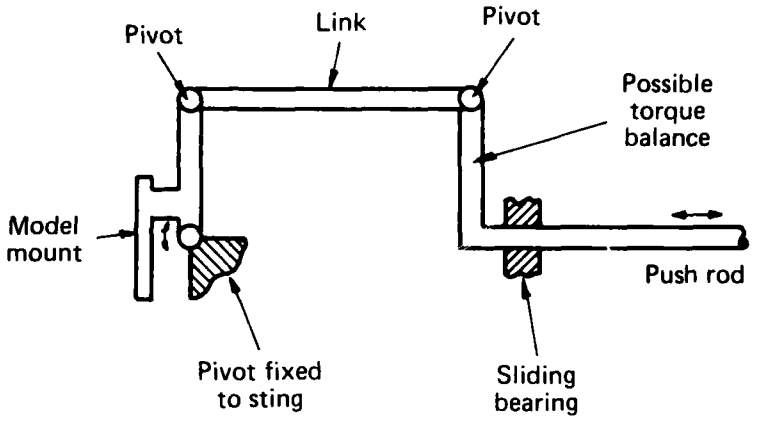

(b) Parallelogram mechanism

FIG 17. MECHANISMS FOR CONVERTING FORCE INTO TORQUE OR LINEAR HARMONIC MOTION INTO ROTARY HARMONIC MOTION

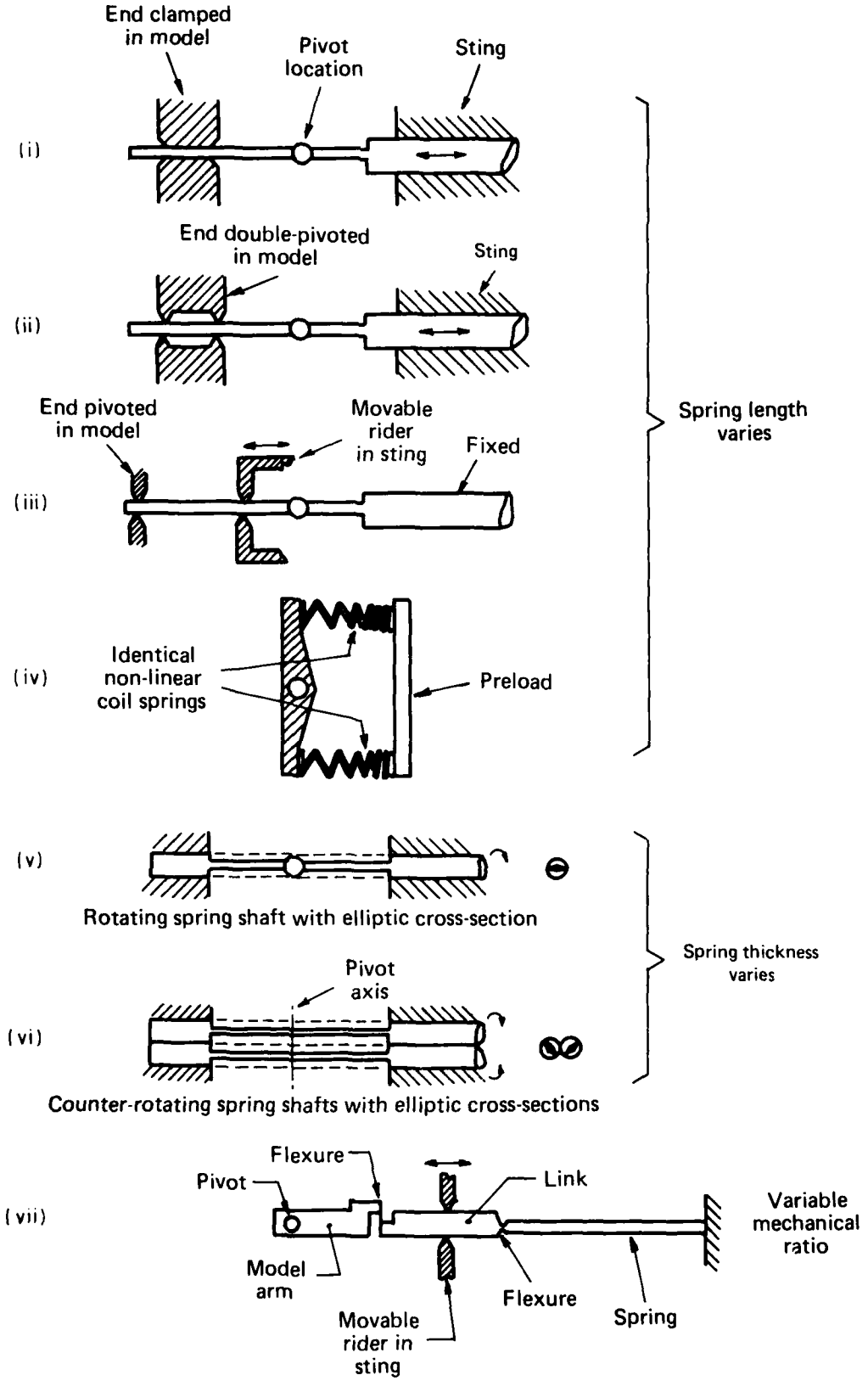

FIG 18. SOME METHODS OF VARYING EFFECTIVE SPRING RATES

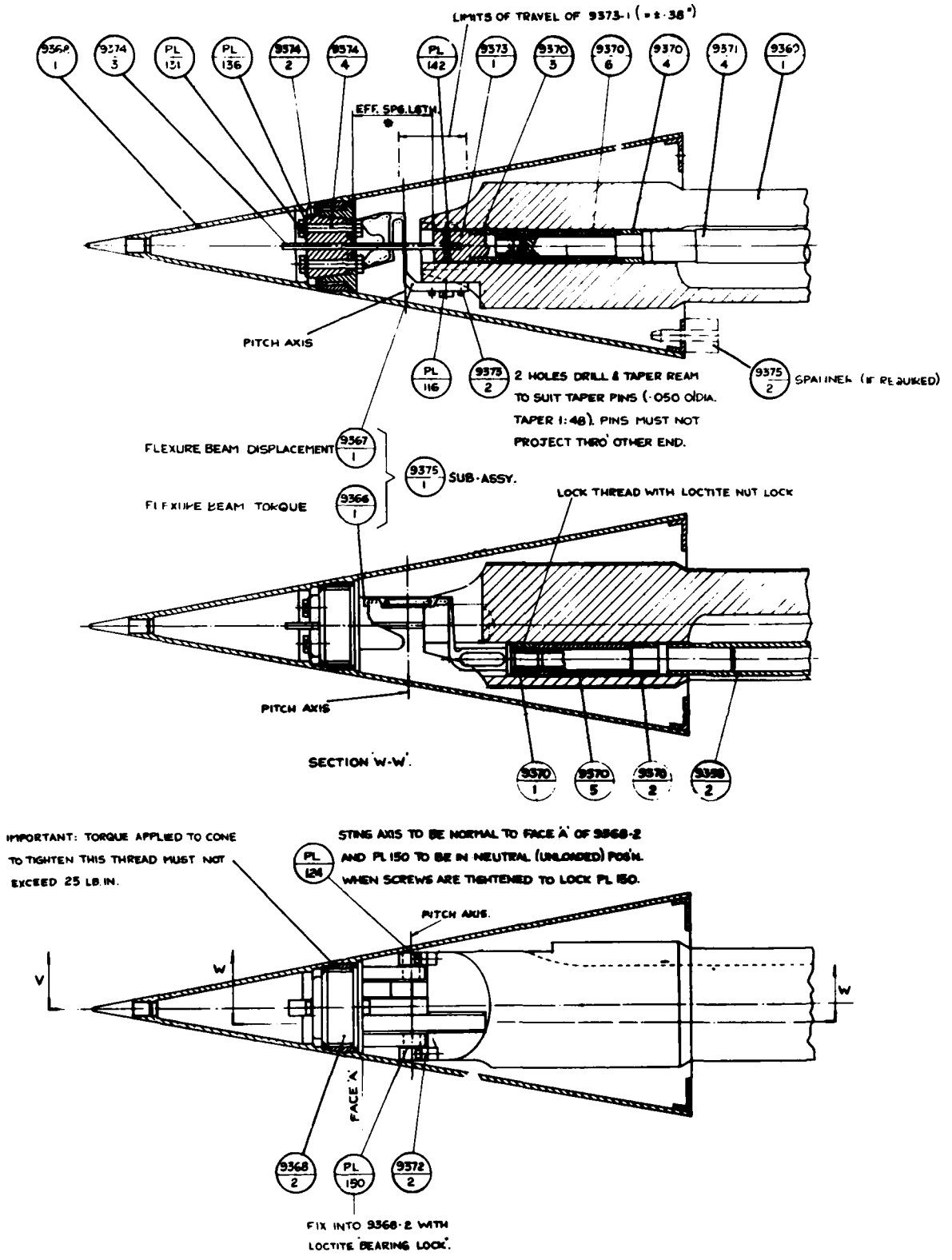
LIMITS OF TRAVEL OF 9373-1 (±·38°)
9369 1
9374 3
PL 131
PL 136
9374 2
9374 4
PL 142
9373 1
9370 3
9370 6
9370 4
9371 4
9369 1
EFF. SPG. LGTH.
PITCH AXIS
PL 116
9378 2
2 HOLES DRILL & TAPER REAM TO SUIT TAPER PINS (·050 OIDIA. TAPER 1:48). PINS MUST NOT PROJECT THRO' OTHER END.
9375 2
SPACER (IF REQUIRED)
FLEXURE BEAM DISPLACEMENT
9367 1
9375 1
SUB-ASSY.
FLEXURE BEAM TORQUE
9366 1
LOCK THREAD WITH LOCTITE NUT LOCK
PITCH AXIS
SECTION 'W-W'.
9370 1
9370 5
9378 2
9368 2
IMPORTANT: TORQUE APPLIED TO CONE TO TIGHTEN THIS THREAD MUST NOT EXCEED 25 LB.IN.
STING AXIS TO BE NORMAL TO FACE 'A' OF 9368-2 AND PL 150 TO BE IN NEUTRAL (UNLOADED) POS'N. WHEN SCREWS ARE TIGHTENED TO LOCK PL 150.
PL 124
PITCH AXIS.
V
W
W
FACE 'A'
9368 2
PL 190
9372 2
FIX INTO 9368-2 WITH LOCTITE 'BEARING LOCK'.

FIG 19.

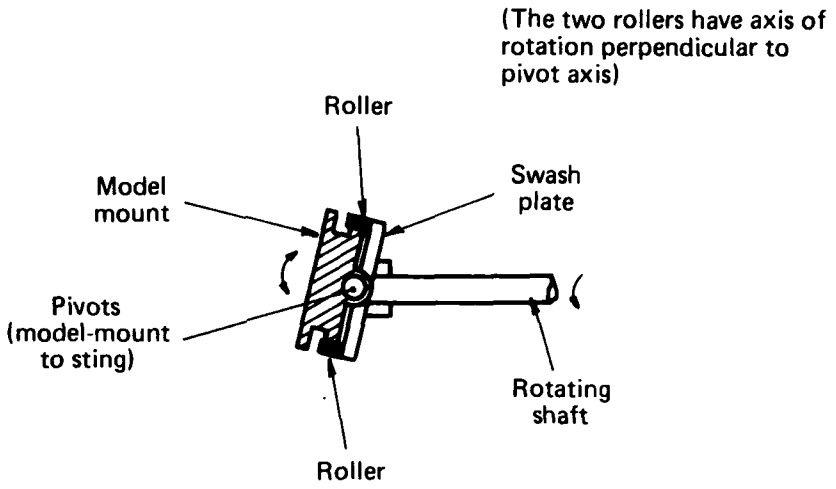

(a) Swash plate mechanism

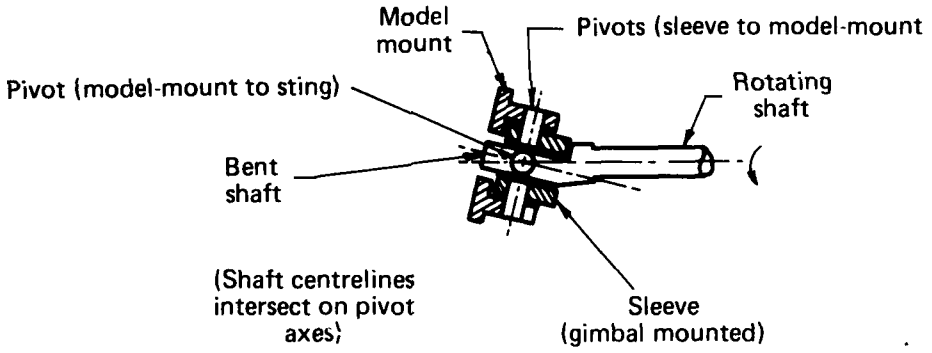

(b) Bent shaft reciprocator

FIG 20. MECHANISMS TO CONVERT ROTATION INTO ROTARY OSCILLATIONS: TWO EXAMPLES SUITABLE FOR LARGER AMPLITUDES

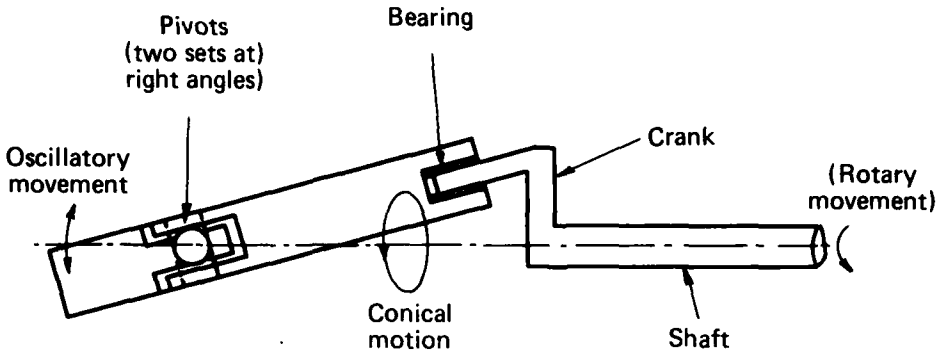

(a) Schematic of a skewed space linkage (deflection exaggerated)

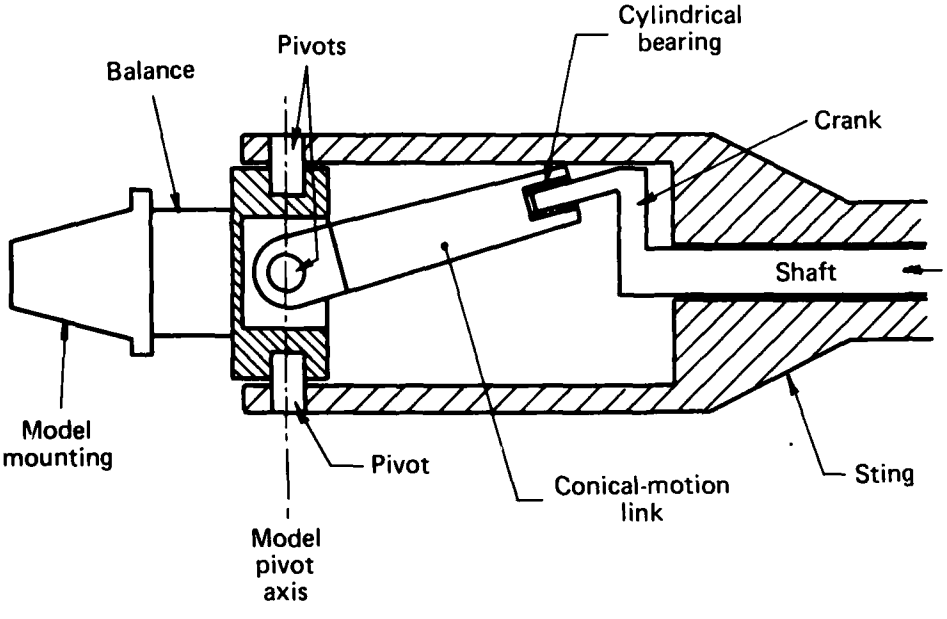

(b) Schematic of a skewed space linkage with balance

FIG 21. RIGIDLY - OSCILLATING SYSTEM USING SKEWED SPACE LINKAGE (CONICAL - MOTION LINK)

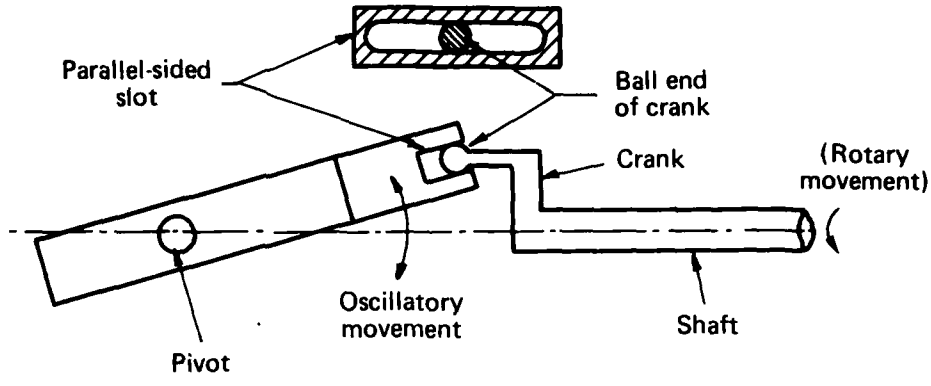

(a) Schematic of a scotch yoke arrangement (deflection exaggerated)

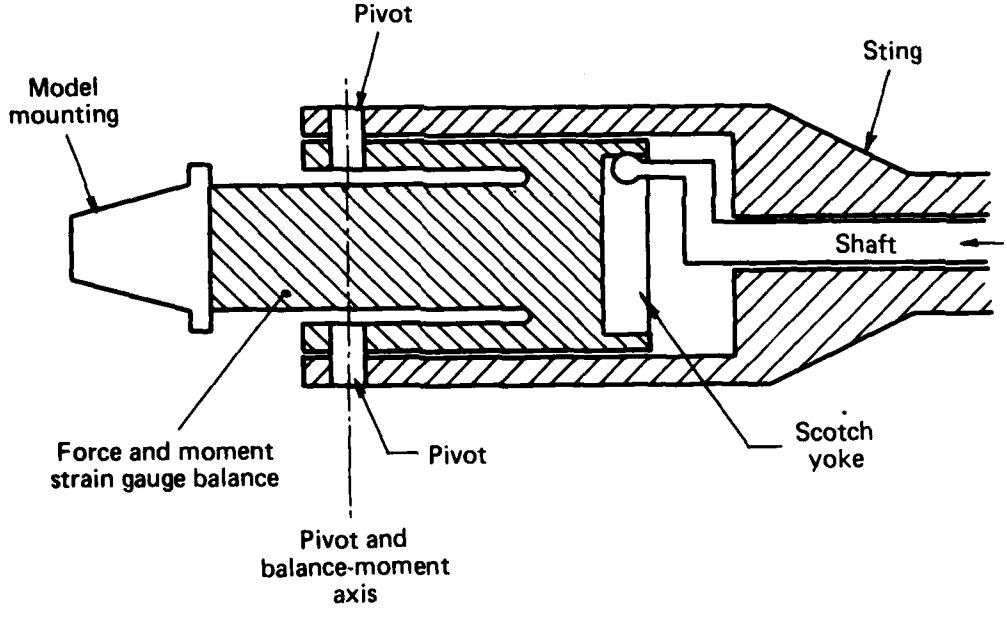

(b) Schematic of a scotch yoke arrangement with balance measuring forces through, and moments about, the pivot axis.

FIG 22. RIGIDLY - OSCILLATED SYSTEM USING SCOTCH YOKE

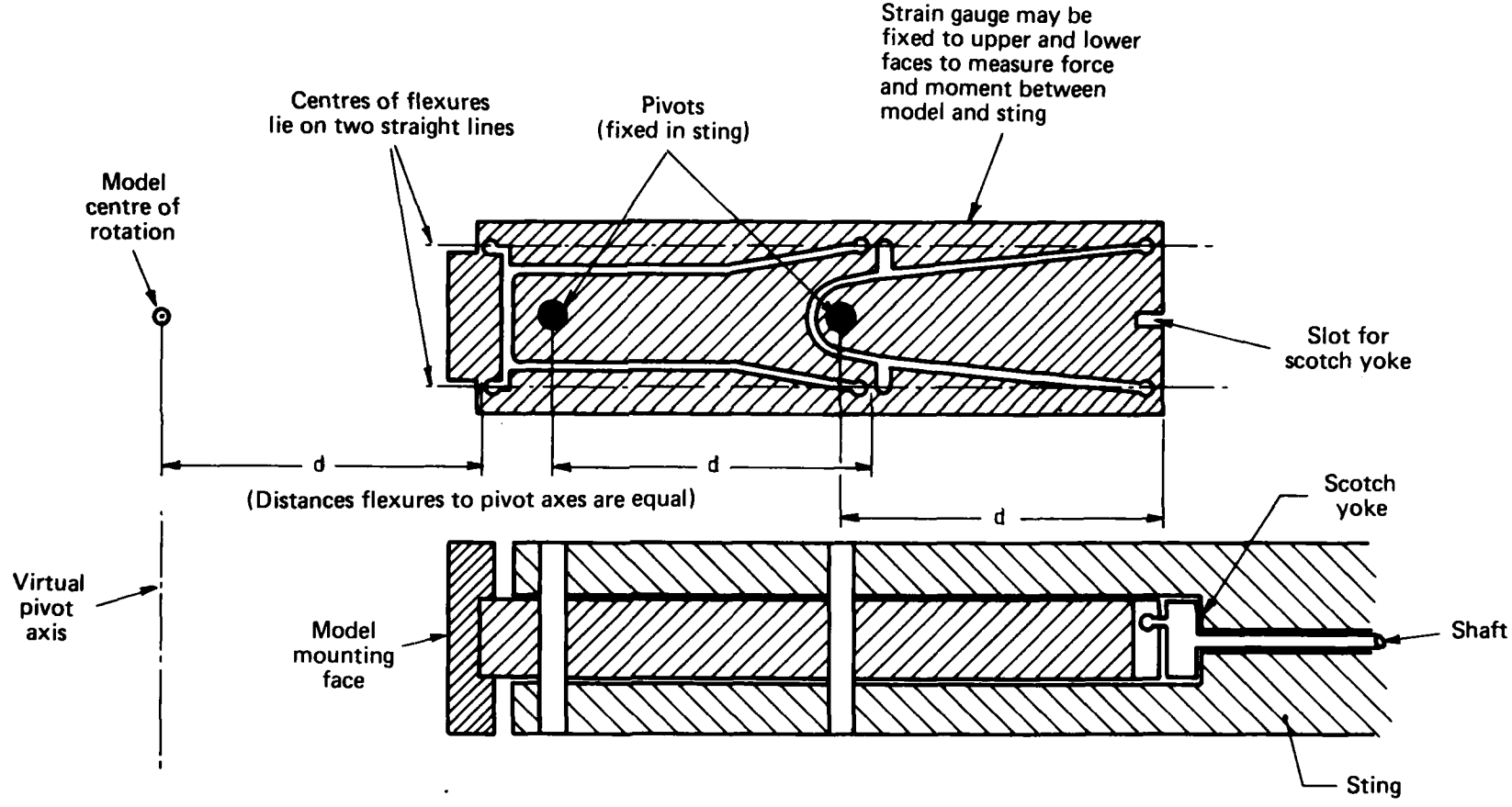

FIG 23. SCHEMATIC OF A RIGIDLY-IMPOSED-OSCILLATION RIG WITH FIXED VIRTUAL PIVOT AXIS

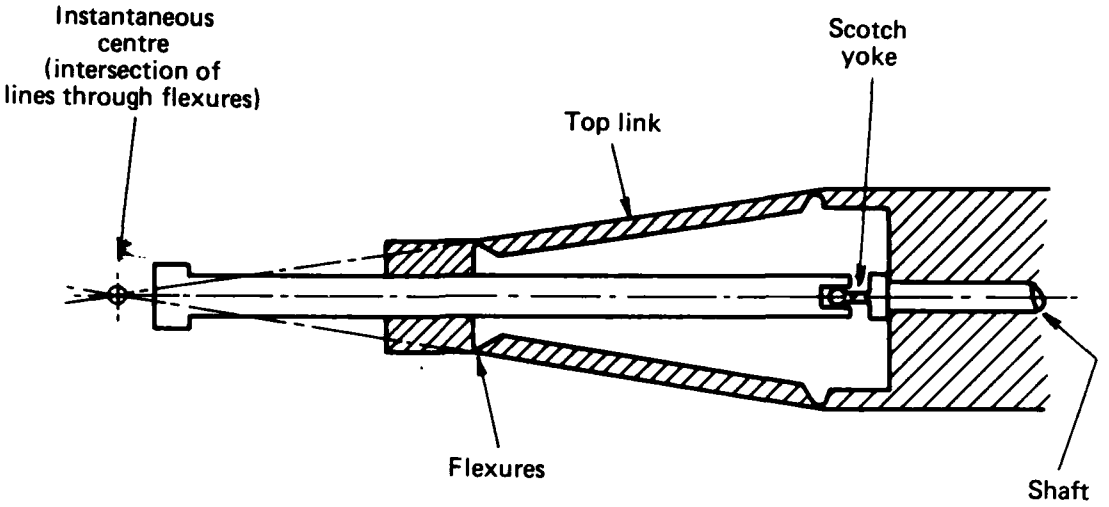

(a) Schematic for zero displacement

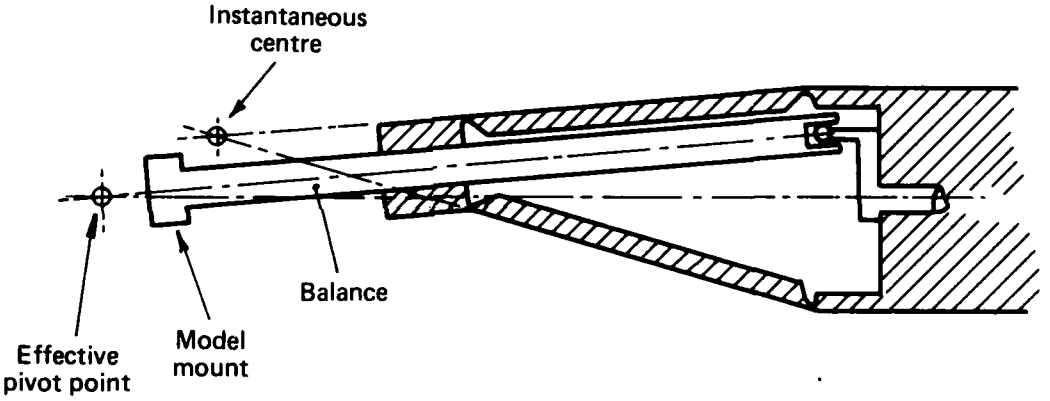

(b) Schematic of rig at maximum (exaggerated) displacement

FIG 24. SCHEMATICS OF APPROXIMATE VIRTUAL-PIVOT RIG

6. METHODS FOR OSCILLATION OF SIDEWALL MOUNTED MODELS

If the model were mounted off one or both of the sidewalls, the problem of cramming the mechanism inside the model and its sting disappears. Three classes of model, full models on struts, half models and two-dimensional aerofoils, are used as are the same three types of exciting mechanism, free oscillation, forced oscillation and rigid drive, used for sting-mounted models.

Figure 8(*c*) shows two possible arrangements for full models on struts. In the second of these arrangements the model strut is attached to a half-model apparatus or to half of a two-dimensional apparatus. This system will be considered as a half model in this discussion although additional tests with just the strut mechanism might be necessary.

The first arrangement of Figure 8(*c*) is unusual in having a moving strut external through the wall of the tunnel. Here as with any sidewall mounted models the oscillation extends right up to the sidewall boundary layer. This might be acceptable for some configurations but is not, in general, a practical idea. Accordingly, a reflection plane is added to the mechanism, and this might either be fixed or rotate with the model. If it rotates, tare (wind-off) readings might be necessary to allow for its effect. If it were fixed some interference with the model motion would still occur but it would be much less than the sidewall effect.

A moving reflection plane becomes a convenient mounting place for the model whether the model is a half-model, two-dimensional aerofoil or a full model on a strut.

For a half model or model on a strut only one such moving reflection plane is needed. Figure 25 shows an arrangement for a forced rig with an electromagnetic shaker providing the power. Inexorable rigs and free oscillation rigs would be similar with the shaker replaced by a rigid drive or simple displacement system respectively. In all cases, the bearings would be required as for the previous section. For free and forced rigs one of the pivots or a separate beam should be strain gauged for a position signal. Detailed design of the torque measuring flexure, which also contributes to stiffness, depends on configuration. For the inexorable rig a balance must be placed between the model and the reflection plane or the model and the shaft.

For a two-dimensional aerofoil, two reflection planes are required. The pivot arrangement now depends on the model type, and the balance arrangement. Figure 26 shows a version of Figure 25 with two pivots on each side and a cross link connecting them outside the tunnel, so that the model is driven from either end. The model itself might be the cross link or it might contain an inner shaft. In this case the model might be effectively driven from one or both ends or the centre. The balances, if required, might be at any of these positions also and might involve only a small span-wise section of the model. (Fig. 27).

In all these cases the model might also be pressure tapped.

It can be seen from the above, that side-wall mounting reduces the mechanical problems but at the expense of reflection plane and tunnel wall interference.

Due to the size of the mechanism involved in side-wall rigs, the inertial terms would be large, and tend to dominate in both the tare and wind on cases for some configurations. This would result in decreased accuracy. Figure 28 shows one way of reducing this problem for a forced oscillation rig. The counter weight is adjusted to have the same moment of inertia as the model-reflection plane-shaft combination.

A similar set up for inexorable (rigid-drive) rigs has the dummy model and model rotating in the same direction with the balance between them, or two balances electrically connected to difference the outputs.

Similar techniques have been used even for sting mounted models going as far as including a dummy model inside the real model but this technique was not considered practical in this size tunnel. Techniques where a remote dummy model is oscillated simultaneously will be considered in a publication on instrumentation.

7. CONCLUSION

Mechanisms have been considered which will allow wind tunnel models to be oscillated in pitch and yaw. Types of pivots, motion producing linkages and connecting linkages have been described as applicable in a 530 by 810 millimetre Transonic Tunnel.

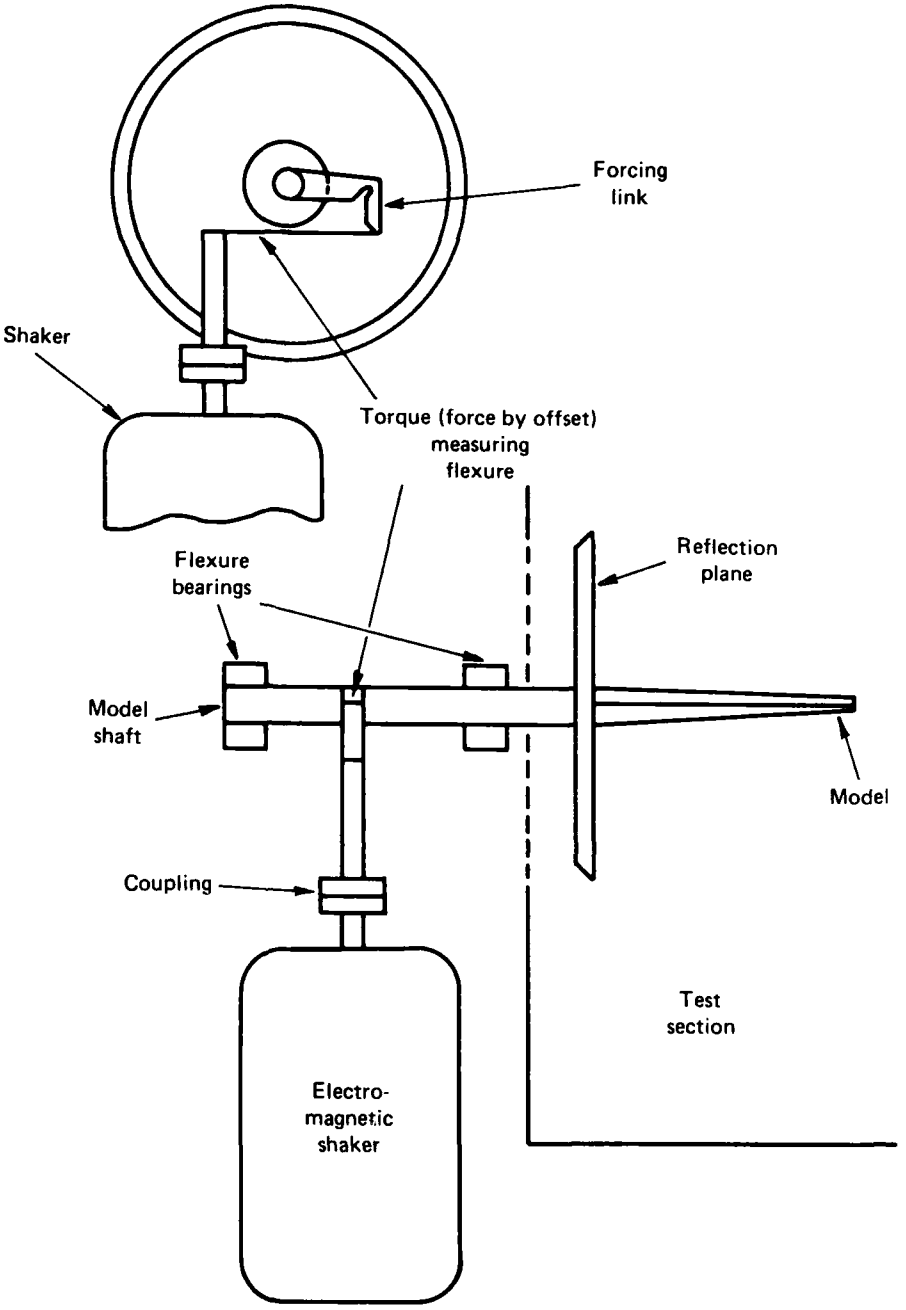

FIG 25 SIDEWALL HALF-MODEL OSCILLATION RIG.

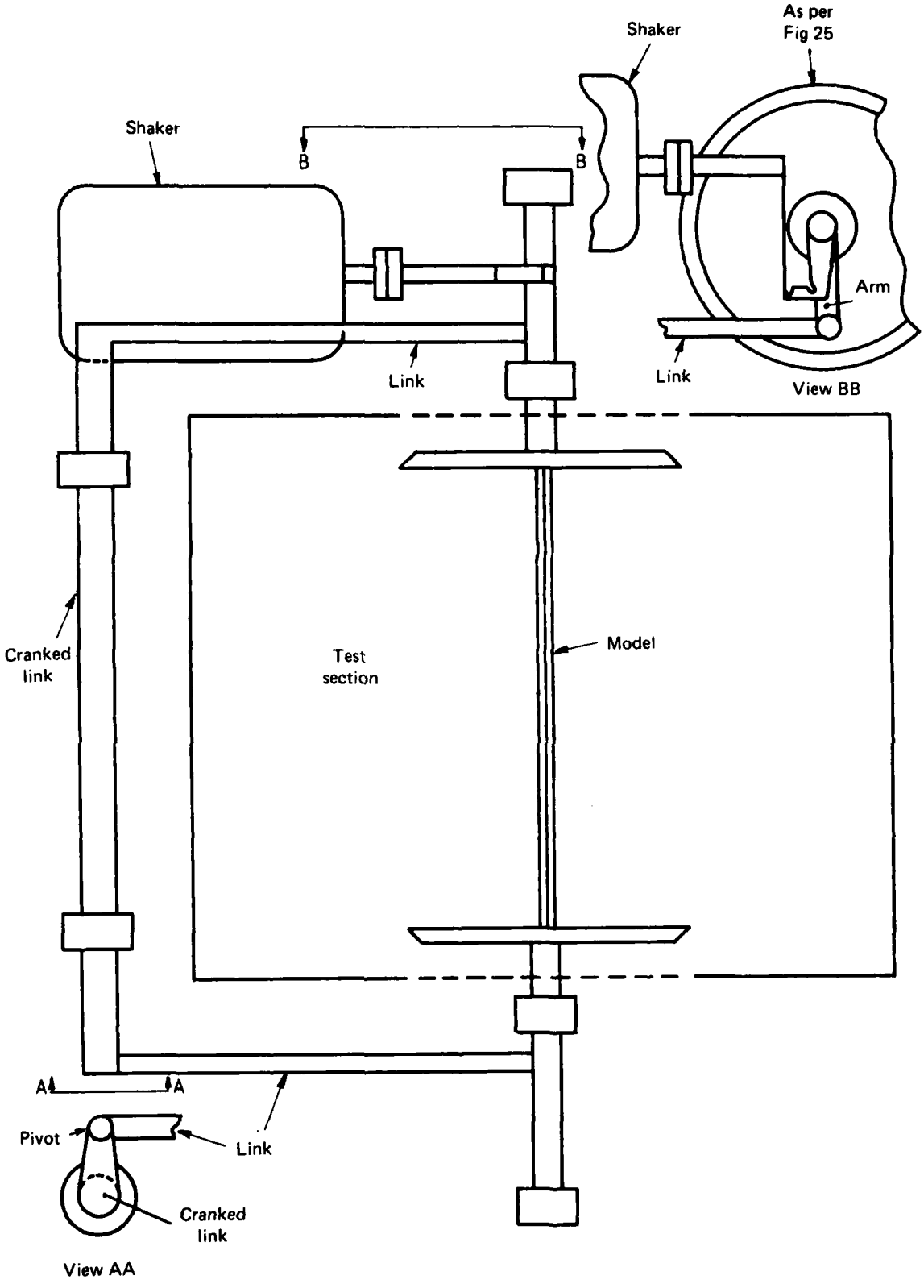

FIG 26. DUAL SIDEWALL RIG FOR TWO DIMENSIONAL MODEL

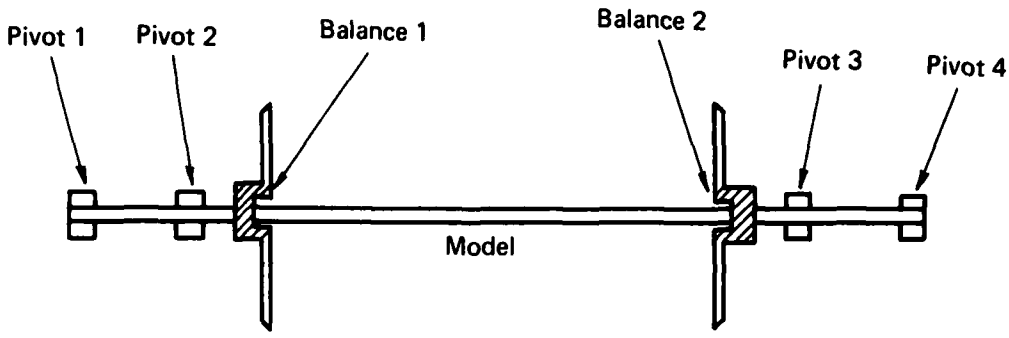

(a) Twin balance arrangements for external cross-link

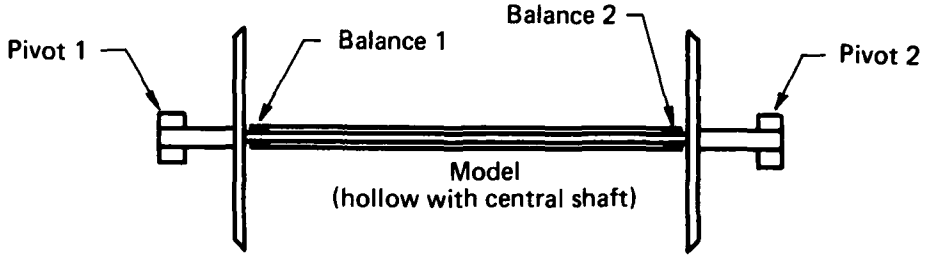

(b) Twin balance arrangement for interal shaft

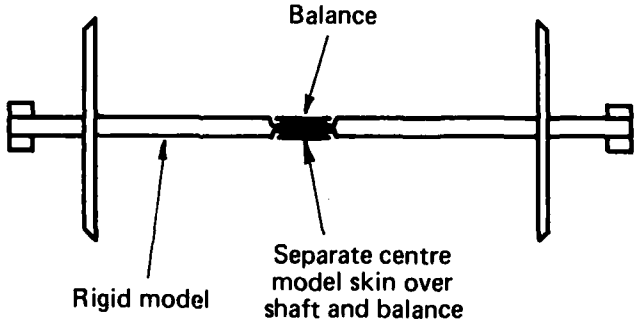

(c) Single balance arrangement for model used as shaft

FIG 27. BALANCE ARRANGEMENTS FOR 2D MODELS

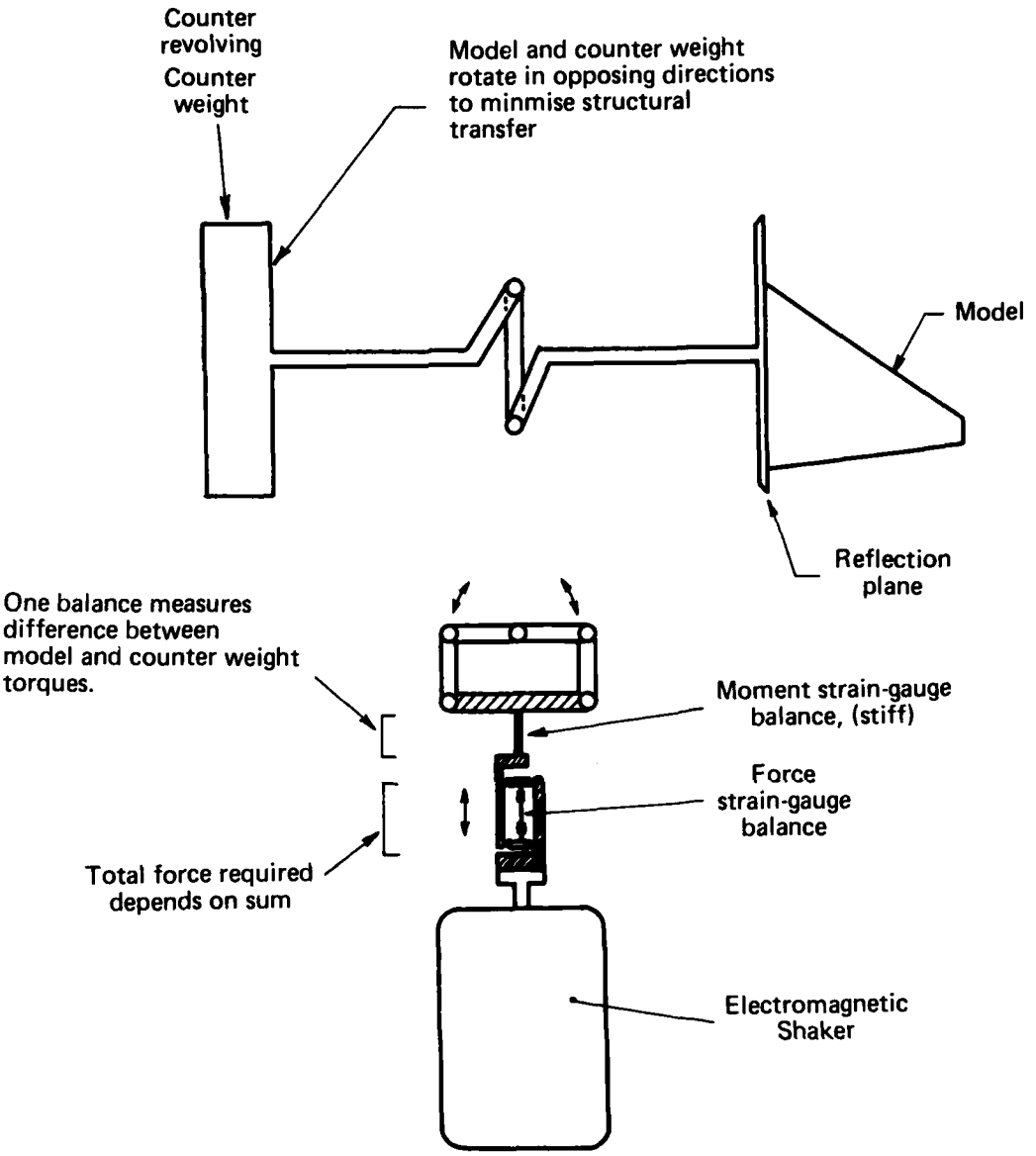

FIG 28. CANCELLING TARE VALUES SIMULTANEOUSLY

TABLE 1

Common Derivatives of the Constant Velocity Set[11] Static Longitudinal Derivatives

* C_{Z_α} Z-force co-efficient due to angle of attack.
* C_{m_α} pitching moment co-efficient due to angle of attack.

Static Lateral Derivatives

* C_{n_β} yawing moment co-efficient due to angle of sideslip.
  C_{l_β} rolling moment co-efficient due to angle of sideslip.
* C_{y_β} Y-force co-efficient due to angle of sideslip.

Dynamic Longitudinal Derivatives

* $C_{m_{\dot\alpha}}$ pitching moment co-efficient due to incidence rate.
* C_{m_q} pitching moment co-efficient due to pitching.
* $C_{Z_{\dot\alpha}}$ Z-force co-efficient due to incidence rate.
* C_{Z_q} Z-force co-efficient due to pitching.

Dynamic Lateral Derivatives

* $C_{n_{\dot\beta}}$ yawing moment co-efficient due to sideslip rate.
* C_{n_r} yawing moment co-efficient due to yawing.
  C_{n_p} yawing moment co-efficient due to rolling.
  $C_{l_{\dot\beta}}$ rolling moment co-efficient due to sideslip rate.
  C_{l_r} rolling moment co-efficient due to yawing.
  C_{l_p} rolling moment co-efficient due to rolling.
* $C_{Y_{\dot\beta}}$ Y-force co-efficient due to sideslip rate.
* C_{Y_r} Y-force co-efficient due to yawing.
  C_{Y_p} Y-force co-efficient due to rolling.

NOTES:

* Measurement of these derivatives is discussed in this Note.

TABLE 2

ARL Transonic Test Facilities

Aerodynamic Data ARL Transonic Wind Tunnel

1. Mach Number Range	0·5 to 1·35 with 0·4 and Mo = 1·4 available under certain conditions.
2. Test Section	Rectangular 808 millimetres high, 533 mm wide and 1930 mm long, with either all four slotted or only top and bottom walls, or combinations of these.
3. Open Area Ratio	With all four walls slotted = 10 percent; top and bottom only = 16 per cent in those faces.
4. Operating Pressure	Starting pressire of the tunnel (atmospheric or less) is limited by the maximum available drive power (2 Megawatts). This limits the maximum dynamic pressure to 21 kilopascal at Mo = 0·5 dropping to 16 kpa at Mo = 1·30.
5. Strain Gauge System	Pollock-Lording AC Solid State Rebalancing type 6 channels.
6. Pressure Measuring System	DC Excitation, Scanivalves (up to 3) with Statham or Bell and Howell bonded gauge pressure transducers, 4 digit plus sign analog to digital integrating converter, multiplexer and controller.
7. Data Reduction:	Digital Equipment PDP8/I with 12k words of core, extended arithmetic element, direct memory access multiplexer, dual 32K discs, dual DECtape transports, Tektronix 611 storage display, Calcomp 565 incremental plotter, Teletype ASR 33 and KSR 43 terminals, Facit 4031 paper tape reader and Potter LP3000 line printer.

REFERENCES
(Bibliography Extract)

Numbers are as in Reference 87

10.	C. J. Schueler, L. K. Ward and A. E. Hodapp	Techniques for Measurement of Dynamic Stability Derivatives in Ground Test Facilities. AGARDograph 121, 1967.
11.	K. Orlik-Rückemann	Methods of Measurement of Aircraft Dynamic Stability Derivatives. N.R.C. of Canada, LR-254, 1959.
19.	F. J. Regan and J. A. Iandolo	Instrumentation, Technique and Analysis Used at the Naval Ordnance Laboratory for the Determination of Dynamic Derivatives in the Wind Tunnel. NOL TR66-23, 1966.
20.	R. C. Maydew and J. C. Weydert	Free-Oscillation Variable-Deflection Dynamic Rig SCR-130, 1959.
55.	C. O. Olsson and K. Orlik-Rückemann	An Electronic Apparatus for Automatic Recording of the Logarithmic Decrement and Frequency of Oscillations in the Audio and Sub-Audio Frequency Range. FFA M52, 1954.
56.	G. F. Forsyth	Calibration and Accuracy Estimation for a Dampometer. ARL Aero. TM 247, 1969.
61.	M. Scherer	Mesure des Dérivées Aérodynamiques en Ecoulement Transsonique et Supersonique ONERA P104, 1962.
64.	C. S. Barnes and A. A. Woodfield	Measurement of the Moments and Product of Inertia of the Fairey Delta 2 Aircraft. RAE TR68160, 1968.
86.	G. F. Forsyth	An Introduction to Dynamic Derivatives: the Concept of Derivatives. ARL AN 330, 1971.
87.	G. F. Forsyth	An Introduction to Dynamic Derivatives (2) the Equations of Motion for Wind Tunnel Pitch-Yaw Oscillation Rigs. ARL AN 377, 1978.
88.	D. J. Foster and G. W. Haynes	Rotary Stability Derivatives from Distorted Models, Journal of the Aeronautical Society, Vol. 60, p. 623.

DISTRIBUTION

Cambridge	Library, Engineering Department	123
	Professor G. K. Batchelor	124
	Professor M. J. Lighthill	125
Liverpool	Professor J. H. Preston, Fluid Mechanics Department	126
London	Professor A. D. Young, Queens College	127
Manchester	Professor, Applied Mathematics	128
	Professor N. Johannessen	129
Nottingham	Library	130
Southampton	Library	131
Strathclyde	Library	132
Cranfield Institute of Technology	Library	133
	Professor Lefebvre	134
Imperial College	The Head	135

UNITED STATES OF AMERICA

NASA Scientific and Technical Information Facility		136
Sandia Group (Research Organisation)		137
American Institute of Aeronautics and Astronautics		138
Boeing Co. Head Office		139
Lockheed Aircraft Co. (Director)		140
McDonnell Douglas Corporation (Director)		141
United Technologies Corporation, Fluid Dynamics Labs.		142
Calspan Corporation		143

Universities and Colleges

Brown (R.I.)	Professor R. E. Meyer, Division of Applied Mathematics	144
California	Dr M. Holt, Dept. of Aeronautics	145
Florida	Mark H. Clarkson, Department of Aeronautical Engineering	146
Harvard	Professor A. F. Carrier, Division of Engineering and Applied Mathematics	147
Illinois	Professor N. M. Newmark, Talbot Laboratories	148
Johns Hopkins	Professor S. Corrsin, Department of Mechanical Engineering	149
Princeton	Professor G. L. Mellor	150
Stanford	Library, Department of Aeronautics	151
George Washington	Library	152
Wisconsin	Memorial Library, Serials Department	153
Brooklyn Institute of Polytechnology	Library, Polytech. Aeronautical Laboratories	154
California Institute of Technology	Library, Guggenheim Aeronautical Laboratories	155
Massachusetts Inst. of Technology	Professor E. Ressner	156

Spares 157–166